estec

European Space Research
and Technology Centre
Keplerlaan 1
2201 AZ Noordwijk
The Netherlands
T +31 (0)71 565 6565
F +31 (0)71 565 6040
www.esa.int

DOCUMENT

ATHENA - Mission Budgets Document

European Space Agency
Agence spatiale européenne

APPROVAL

Title ATHENA – Mission Budgets Document	
Issue 2	**Revision** 2
Author	**Date** 18/10/2017
Approved by	**Date**

CHANGE LOG

Reason for change	Issue	Revision	Date
Initial issue.	1	0	12/06/2014
Update to include non-x-ray particle background, absolute time accuracy and pointing requirements, and also general update.	1	1	20/08/2014
Included background update, and also placeholders for calibration of effective area. General update throughout.	1	2	26/02/2015
Update for industrial KO, on basis of: • Mission Operational Availability increase to 85% • Introduced placeholder for PSF HEW • Corrected small errors throughout	1	3	07/07/2015
Update #2 version – minor corrections, added FoV and effective area loss, SC op. av. Down to 90%	1	4	06/10/2015
Post MCR update	2	0	10/06/2016
Post document numbering system update	2	1	07/09/2017
Pre Prime Phase A CR update	2	2	18/10/2017

CHANGE RECORD

Issue 2	**Revision** 0		
Reason for change	**Date**	**Pages**	**Paragraph(s)**
Updated the document reference number and the reference numbers of the affected ADs and RDs	07/09/2017		
Reason for change issue 2.0	**Date**	**Pages**	**Paragraph(s)**

MCR Update: Added PSF placeholder (overall PSF including pixel sampling – for completion by the ASST) Re-wrote Effective Area and Grasp section to remove baseline (small mirror) case and make clear that all effects are now under Prime responsibility (Mirror Area inc. internal effects, Mirror misalignment ref. LoS, LoS error, contamination) with examples only. Tightened AKE requirement (ASST justification received). Replaced RPE with RKE in pointing section, and relevance to HKE budget. Updated dV budget on the basis of MCR-consolidated budget, fixed noise value and including margins. Removed LV performance section – all information on LV, inc. performance, in the LS IRD.			
Issue 2.2: Returned the SC to the smaller 15-row mirror specification Improved the requirement break-down for A_eff (removed 'target' from the specification, now just on-axis) Net Observing Time breakdown included TBDs (no MOP available for new 4 year mission). Removed Effective Area calibration – will be handled by separate calibration plan and requirements – see Product Tree update.	Throughout		

Table of contents:

ACRONYMNS

CCDS	Consultative Committee for Space Data Systems
CDMU	Central Data Management Unit
ERT	Earth Reception Time
ESOC	European Satellite Operations Centre
GPS	Global Positioning System
GS	Ground Station
HEO	Highly Eccentric Orbit
L2	2nd Lagrangian point (orbit)
OBDH	On Board Data Handling
OBT	On Board Time
ODF	Observation Data File
QLA	Quick Look Analysis
RXTE	Rossi X-ray Timing Explorer
TAI	Time Atomic International
TT	Terrestrial Time
UTC	Universal Time Coordinated

1 INTRODUCTION & SCOPE

This document is the repository for the Mission-level performance breakdown and budgets, and is an instantiation of the Technical Budget standard DRD (Annex I of [AD01]), as part of the Mission DDF (DDF_1.0).

Regarding the flow-down of quantified requirements from the SciRD [RD01] and ConOps [RD07], via the MRD [RD02] to one of the tier-1 Product Tree [RD03] items, there are two cases:

1. A requirement is flown directly down to, and accordingly is the responsibility of, a single tier-1 product without decomposition/translation; in this case, the top-level budget for this requirement is the responsibility of the tier-1 product supplier, and will appear in the budget document associated with that product.
2. A requirement translation to one or more tier-1 products, or a requirement decomposition among two or more tier-1 products, is necessary; in this case, the top-level budget is the responsibility of the ESA PO, and is maintained in this document.

This document deals with the second case, and presents the budgets and models controlling the decomposition and/or translation of MRD requirements into engineering requirements allocated to tier-1 products in their respective specifications.

1.1 Decomposed Mission Requirements

This document also currently contains two decompositions from the SciRD to the MRD which are the responsibility of the ASST:

- Net observing times
- GRB trigger efficiency

The following MRD/ConOps requirements are decomposed to tier-1 product specifications in this document:

- PSF HEW
- Operational availability
- Mission Reliability
- Effective Area & Grasp
- Field of View
- Effective Area calibration
- ToO reaction time
- Science telemetry latency
- Absolute time accuracy
- Non x-ray particle background
- Astrometry and SC (telescope) pointing

- Delta V (station-keeping).

Note: The decompositions are depicted graphically using colour coded box diagrams. Where appropriate, and for information only, the derived requirements used in the CDF study for the SC are presented as boxes with dashed-lines.

1.2 Applicable Documents

[AD01] Space engineering: System engineering general requirements, ECSS-E-ST-10C, Issue 3.0, 06/03/2009.

[AD02] Space Product Assurance: Availability analysis, ECSS-Q-ST-30-09C, Issue 2.0, 31/07/2008.

1.3 Reference Documents

[RD01] ATHENA - Science Requirements Document (SciRD), ESA-ATHENA-ESTEC-SCI-RS-0001, Issue 1.0, 12/06/2014.

[RD02] ATHENA - Mission Requirements Document (MRD), ESA-ATHENA-ESTEC-MIS-RS-0001, Issue 1.0, 12/06/2014.

[RD03] ATHENA - Product Tree, ESA-ATHENA-ESTEC-MAN-PT-0001, Issue 1.0, 12/06/2014.

[RD04] ATHENA+: ATHENA+ Response Files, ECAP-ATHENA+-20130325, 25/03/2013.

[RD05] IXO baseline design report, IXO-TASF-RP-004, Issue 4.0, 30/07/2010.

[RD06] Space Debris Mitigation for Agency Projects. ESA/ADMIN/IPOL (2008), 1st April 2008, Annex 1 and 2.

[RD07] ATHENA – Concept of Operations, ESA-ATHENA-TN-0005, Issue 1.0, 11/09/2013.

[RD08] ATHENA - ToO Reaction Architecture Trade-off, ATHENA-ESA-TN-0002, Issue 1.0, TBW.

[RD09] ATHENA: The Advanced Telescope for High Energy Astrophysics: Mission Proposal, K Nandra et al 2014

[RD10] IXO Environmental Specification, Sørensen, J., Rodgers, D., Drolshagen, G., Santini, G., 2010

[RD11] Estimate of the impact of background particles on the X-ray Microcalorimeter Spectrometer on IXO, Nucl. Instrum. Methods Phys. Res. Sect. Accel. Spectrometers Detect. Assoc. Equip. 686, 31–37, Lotti, S., Perinati, E., Natalucci, L., Piro, L., Mineo, T., Colasanti, L., Macculi, C., 2012

[RD12] A magnetic diverter for charged particle background rejection in the SIMBOL-X telescope, in: Turner, M.J.L., Flanagan, K.A. (Eds.), p. 70112Y–70112Y–11. doi:10.1117/12.789917, Spiga, D., Fioretti, V., Bulgarelli, A., Dell'Orto, E., Foschini, L., Malaguti, G., Pareschi, G., Tagliaferri, G., Tiengo, A., 2008

[RD13] ATHENA Payload Definition Document, ASST, 2014

[RD14] X-IFU consortium inputs to the ATHENA L2 Payload Definition Document Update, CNES, IRAP, 2014

[RD15] Timing accuracy and capabilities of XMM-Newton M. G. F. Kirsch et al Proc SPIE Vol. 5165 2004

[RD16] XMM Timing he relative and absolute timing accuracy of the EPIC-pn camera on XMM-Newton, from X-ray pulsations of the Crab and other pulsars A. Martin-Carrillo et al A&A 545, A126 (2012)

[RD17] *INTEGRAL* timing and localization performance R. Walter (arXiv:astro-ph/0309525v1)

[RD18] E. Serpell and F. Possanzini, *XMM-Newton Time Correlation,* XMM-OPS-RP-0026-TOS-OF Issue 1, 2003

[RD19] Absolute timing with IBIS, SPI and JEM-X aboard INTEGRAL. Crab main-pulse arrival times in radio, X-rays and high-energy gamma -rays , Astronomy and Astrophysics, v.411, p.L31-L36 L Kuiper, et al. Astronomy and Astrophysics, v.411, p.L31-L36 2003 (arXiv:astro-ph/0309178)

[RD20] Absolute Timing of the Crab Pulsar with the Rossi X-Ray Timing Explorer, A Rots et al. The Astrophysical Journal, Volume 605, Issue 2, pp. L129-L132, 2004 (arXiv:astro-ph/0403187)

[RD21] Jodrell Bank Crab Pulsar Monthly Ephemeris http://www.jb.man.ac.uk/pulsar/crab.html

[RD22] IXO AOCS Analyses. TEC-ENC/40.10. Issue 1.1, 27/09/2010.

[RD23] ATHENA_L1 Internal Study Report. SRE-PA/2011.033/NR. Issue 1.0, 22/06/2011.

[RD24] XMM NEWTON – Performance assessment of the XMM NEWTON Star Tracker and the On-Ground Attitude Reconstruction Process. Ref XMM-MOC-TN-0141-TOS-GFT 11/02/2004.

[RD25] ATHENA+ – CreMA. Issue 1.0, MAS Working Paper No. 598, 12/06/2014.

[RD26] ATHENA – L2 Proposal.

[RD27] ATHENA – Mock Observing Plan, TO BE UPDATED.

[RD28] ATHENA – Reference Telescope Design, ESA-ATHENA-ESTEC-PL-DD-0001, Issue 2.2.

[RD29] The Optical Design of the ATHENA+ Mirror: ATHENA+ Supporting Paper.

[RD30] Draft Programme Proposal on the Ariane Launcher Development Programmes for decision at CM-14, ESA/PB-LAU(2014)48, rev. 1, Annexes A and B, 17/10/2014.

[RD31] A5 User Manual Addendum: Modification of the Shock specification and the Shock qualification methodology. DC/BD/ST/JTH/MBe/L13.198.

[RD32] XMM-Newton Quarterly Mission Status & Performance Indicators, http://xmm.esac.esa.int/external/xmm_news/mission_status/index.php

[RD33] XMM-Newton Target of Opportunity (ToO), http://xmm.esac.esa.int/external/xmm_sched/too/index.php.

[RD34] Bonino, L., 2010. Preliminary instrument module contamination control plan (report n. 8).

[RD35] Collon, M., 2010. High-Performance X-ray optics. Abstract and Summary Report.

[RD36] Ferreira, D.D.M., Christensen, F.E., Jakobsen, A.C., Westergaard, N.J., Shortt, B., 2012. ATHENA optimized coating design, in: Takahashi, T., Murray, S.S., den Herder, J.-W.A. (Eds.), p. 84435L. doi:10.1117/12.925694

[RD37] Nandra, K., Barcons, X., Herder, J.-W. den, Barret, D., Fabian, A., Piro, L., 2013. ATHENA mission proposal.

[RD38] Oosterbroek, T., 2010. IXO Telescope and Mirror Assembly Reference Document.

[RD39] Oosterbroek, T., 2011. IXO: Molecular contamination on the mirror.

[RD40] Rando, N., 2010. Assumptions for estimating the effective area of the IXO telescope.

[RD41] Wille, E., 2011. ATHENA Mirror Module Design and Development Status.

[RD42] Willingale, R., Pareschi, G., 2013. The optical design of the Athena+ mirror.

[RD43] ATHENA – Operational aspects of response to ToO alerts and return to routine timeline activities, ESA-AMCO-MO-003, 31/03/2016.

[RD44] ATHENA – SWG2-1-TN-0003: Positional accuracy requirements for TP2.1 (high-z AGN), Issue 1.0, 14/04/2016.

2 POINT SPREAD FUNCTION HEW

2.1 MRD Requirements

ID	Requirement
Angular Resolution	
R-MIS-320	The ATHENA Mission shall perform Narrow Field observations with a Point Spread Function (PSF) having ≤TBD" Half Energy Width (HEW) at the target, over an energy range of 0.1 - 6keV.
R-MIS-321	The ATHENA Mission shall perform Wide Field observations with a Point Spread Function (PSF) having ≤TBD" Half Energy Width (HEW) at the target, over an energy range of 0.1 - 6keV.
R-MIS-322	The ATHENA Mission shall perform Fast Chip observations with a Point Spread Function (PSF) having ≤TBD" Half Energy Width (HEW) at the target, over an energy range of 0.1 - 6keV.
R-MIS-340	The ATHENA Mission shall perform all observations with a Point Spread Function (PSF) having ≤20" HEW at the target, over the energy range 6 - 15 keV.
R-MIS-350	The ATHENA Mission shall perform all observations, at 25' off-axis, with a Point Spread Function (PSF) having ≤10" HEW, over the energy range 0.1-6keV.

2.2 Decomposition

TBW by the ASST (taking into account the SC-provided PSF and the sampling of the instruments as a function of pixel size, for both requirement and goal).

2.3 Derived Requirements

The initial decomposition is shown in the following figure.

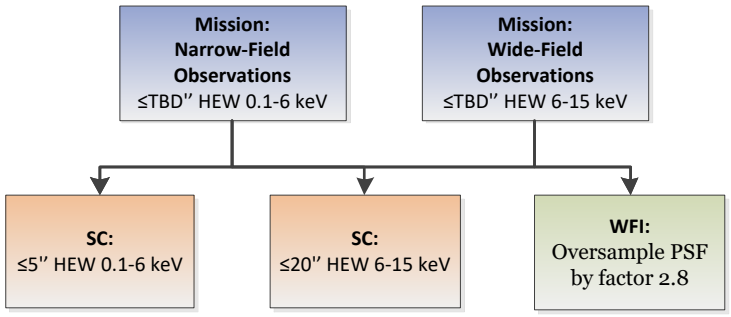

Figure 1: Decomposition of PSF HEW

3 OPERATIONAL AVAILABILITY

3.1 MRD Requirement

ID	Requirement
R-MIS-870	The ATHENA Mission shall provide an operational availability of the science data product of greater than 85% averaged over the NoP and EoP.

Contingencies	Includes: a) time lost due to ground segment problems (slew parameters not computed in time, transmission drops, ground station antenna or link problems…) b) time lost because of spacecraft problems c) time lost due to instrument anomalies d) time not used because of Ground Station support to other spacecraft
Overheads	Time spent to configure the instruments at the start and end of each observation/exposure.
S/C-activities	Time where no activity could be scheduled. Such as planned tests, maintenance or calibration of star tracker, fine Sun Sensor, thruster torque etc. Extra post-slew margins requested for a few special manoeuvres. Problems with ground-station handovers. Special instrument tests that need to be manually commanded are also included here.
Slews	Time spent slewing between targets (includes star tracker field acquisition and locking on a guide star)
High radiation events	time lost due to high radiation coming from the sun (solar flares) or other sources (cosmic rays)

3.2 Decomposition

Note: this decomposition has been performed in BlockSim.

The operational availability requirements impact the ATHENA system as a whole (i.e. space, operational, and science segments). Therefore, an apportionment needs to be performed at lower level (Product Tree tier-1) such that the operational availability requirements are met for the science data products.

To perform the availability apportionment at tier 1 level, ATHENA is modelled as a series system. The apportionments take into account for each block an estimated static availability, the maximum achievable availability, and a predefined feasibility (easy, moderate, or hard) to achieve that level of availability. In addition, we need to specify the 'availability' of the environment, i.e. make an apportionment for when solar activity & GCRs is preventing observations (increased background).

Figure 2: Availability Block Diagram for Type_1 Science Data (environment not shown)

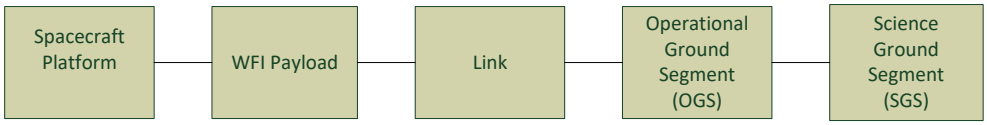

Figure 3: Availability Block Diagram for Type_2 Science Data (environment not shown)

In order to estimate the expected high-radiation ('environment') periods for ATHENA, values from the best (2014 Q3 – 0.95%) and worst case (2004 Q2 – 4.38%) quarters of XMM Newton data were used [RD32]. This leads to a reasonable allocation of 3%.

Tier-1 Product	Est. Operational Availability	Est. Maximum Achievable Operational Availability	Est. Pre-defined Feasibility	Optimum Apportionment
Environment	0.97	0.97	-	0.97
SC	0.85	0.9	Moderate	0.9
X-IFU	0.9	0.95	Hard	0.98
Link	0.99	0.9999	Moderate	0.999
OGS	0.95	0.999	Moderate	0.998
SGS	0.98	0.999	Hard	0.997
Type_1 Av.	0.68			0.85

Table 1: Tier 1 Availability Apportionment for Type_1 Science Data (Narrow Field)

Tier-1 Product	Est. Operational Availability	Est. Maximum Achievable Operational Availability	Est. Pre-defined Feasibility	Optimum Apportionment
Environment	0.97	0.97	-	0.97
SC	0.85	0.9	Moderate	0.9
WFI	0.9	0.95	Hard	0.98
Link	0.99	0.9999	Moderate	0.999
OGS	0.95	0.999	Moderate	0.998
SGS	0.98	0.999	Hard	0.997
Type_2 Av.	0.68			0.85

Table 2: Tier 1 Availability apportionment for Type_2 Science Data (Wide Field & Fast-Chip)

3.3 Derived Requirements

The decomposition is shown in the following figure.

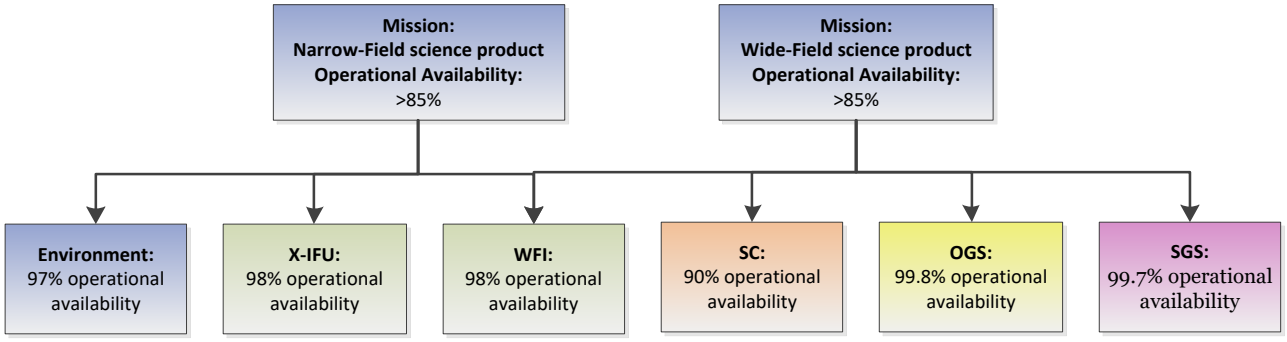

Figure 4: Decomposition of Operational Availability

Note: The defined availabilities for the instruments are with respect to their scheduled periods of observation, i.e. the X-IFU availability does not take into account the cooling-cycle, when the WFI will be observing.

4 NET OBSERVING TIMES

4.1 SciRD/ConOps Requirements

Note: this section will be updated once the new MOP is available.

We define two observation types:

- Type_1: Narrow-Field observations (to be performed with X-IFU)
- Type_2: Wide-Field observations (to be performed with WFI.)

Furthermore, in accordance with the Mock Observing Plan [RD27] we can categorise each observation type as containing the following categories:

- Category A observations: pursuing core science requirements
- Category B observations: pursuing core science goals
- Category C observations: pursuing observatory science requirements
- Category D observations: pursuing observatory science goals.

The following table (derived from the Mock Observing Plan) summarises the requirements and goals (in the SciRD) on net observing times for the four observation categories associated with each type, e.g. in the case of WFI category A:

$$t = \sum_{i=1}^{n} t\_WFI\_catA_i$$

Table 3: Narrow/Wide-Field observation net observing times by category from the Mock Observing Plan

	Category	Net time required [ks]
Narrow-Field	A	TBD
	B	TBD
	C	TBD
	D	TBD
Wide-Field	A	TBD
	B	TBD
	C	TBD
	D	TBD

We sum the core (A, C) and observational (B, D) categories together to derive the required and goal net observing times for Narrow-Field and Wide-Field observations. This is then increased by 5% to represent an allocation of time to calibration activities. This leads to the Mission requirements summarised in the following table.

Note: we assume meeting core & observatory science requirements is necessary to complete the Mission.

Table 4: Narrow/Wide-Field net observing time requirements/goals as declared in the MRD, including 5% calibration time

Category	Net time required [ks]
X-IFU core & obs requirement [ks]	TBD
X-IFU core & obs goal [ks]	TBD
WFI core & obs requirement [ks]	TBD
WFI core & obs goal [ks]	TBD

From the ConOps, the operational mission is split into Nominal and Extended Operational Phases (NoP/EoP) – the NoP is required to satisfy the net observing time requirements, whereas the EoP is required to satisfy the net observing time goals.

4.2 Decomposition

Under the assumption that the SC is successfully delivered into the operational orbit and fully commissioned, meeting the net observing time requirements (during the NoP) and goals (during the EoP) will depend upon the availability of the ATHENA mission to perform science operations and produce the final science data product. The operational availability requirement is placed on the science data products as these are the ultimate mission product encompassing the entire system chain.

The decomposition/translation is from the net observing times specified in the SciRD to (i) an overall ATHENA science data product availability (split into Narrow and Wide-Field products), and (ii) NoP and EoP durations, specified in the MRD.

The ATHENA science data product availability (A_0) is defined as an operational mean availability in accordance with [AD02]. This covers all possible sources of downtime and represents the average percentage of time that the science data product is available over the operating cycle.

$$A_0 = \frac{Uptime}{Operating\ Cycle}$$

Operational availability is a demonstrated (*a posteriori*) availability measure based on actual operational data. However, in the frame of the ATHENA project it shall be understood as the expectation of the science community in order to satisfy the scientific requirements of the mission.

We define the operating cycles for the Narrow-Field and Wide-Field observations as being the sum of those periods of the mission that are allocated to Narrow or Wide-Field observations.

Note: A_0=85% is considered an achievable number based upon previous IXO studies.

We define the operational availability requirements as:

- The operational availability of the Type_1 & Type_2 science data products shall be better than 85% averaged over the mission lifetime, i.e.:

$$A_{o\ type\_1} \geq 0.85$$

Note: The allocation of 78% for Type_1 science data product implies that, during the X-IFU CC down-time, the instruments are swapped over and WFI performs observations.

Only temporary random and deterministic system outages shall be considered as sources of downtime for the purpose of the operational availability computation. Examples of such temporary outages include but are not limited to:

- Random events: Weather related events; momentary service interruption after failure of nominal unit, single/multiple event upsets (SEU), or during system reconfiguration (e.g. switch to redundant unit) or re-initialization of the same unit (e.g. after SEU).
- Deterministic events: Science target acquisitions; payload calibrations; station keeping manoeuvres, etc.

Definitive system failures (reliability) shall not be considered.

Nominal (NoP) and extended (EoP) mission durations can then be derived from the observational requirements and the availability requirements as follows:

$$\frac{R_{type\_1}}{A_{0\ type\_1}} = NoP\_duration_{type\_1}$$

$$\frac{R_{type\_2}}{A_{0\ type\_2}} = NoP\_duration_{type\_2}$$

$$NoP\ duration = NoP\_duration_{type\_1} + NoP\_duration_{type\_2}$$

$$\frac{G_{type\_1} - R_{type\_1}}{A_{0\ type\_1}} = EoP\_duration_{type\_1}$$

$$\frac{G_{type\_2} - R_{type\_2}}{A_{0\ type\_2}} = EoP\_duration_{type\_2}$$

$$EoP\_dur = EoP\_duration_{type\_1} + EoP\_duration_{type\_2}$$

This results in the following NoP/EoP duration requirements.

Table 5: Summary of NoP/EoP duration requirements

TBD

4.3 Derived Requirements

The decomposition is shown in the following figure. Given the requirements expressed in the Observing Plan, and under the assumption that the operational availability requirements are met, a 3.5 (rounded to 4) year mission is be sufficient to meet core and observatory science requirements, and 0.8 (rounded to 1) extra year is sufficient to meet goals for core and observatory science.

TBD

Figure 5: Net observing time decomposition

5 MISSION RELIABILITY

5.1 MRD Requirement

ID	Requirement
R-MIS-20	The ATHENA Mission shall have a reliability (probability of continued successful delivery of both Narrow and Wide-Field observation data products to the end user) at the end of the NoP of 75%.

5.2 Decomposition

The reliability requirements impact the ATHENA system as a whole (i.e. space, operational, launch and science segments). Therefore, an apportionment needs to be performed at lower level (Product Tree tier-1) such that the overall reliability requirement is met.

Tier-1 Product	Apportionment
SC	0.90
X-IFU	0.90
WFI	0.95
OGS	1.00
SGS	1.00
LS	0.98
Narrow Field	**0.80**
Wide Field & Fast	**0.85**
Overall	**0.75**

Table 6: Tier 1 reliability apportionments for X-IFU, WFI and overall

5.3 Derived Requirements

The decomposition is shown in the following figure.

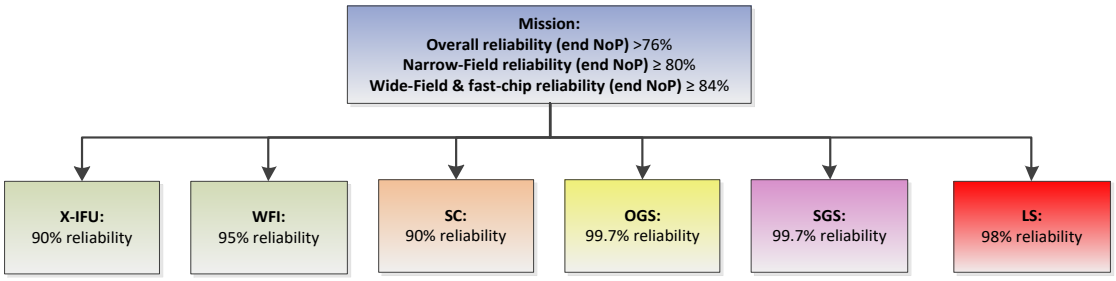

Figure 6: Decomposition of reliability

6 GRB TRIGGER EFFICIENCY

6.1 SciRD Requirement

SG4.1: 40 narrow-field observations of distant GRBs for 50ks.

Note: no confidence-level has been associated with this requirement, but the implication is 50% cl. Poisson statistics would need to be used to attach a cl to the requirement.

6.2 Decomposition

GRB alerts are a subset of ToO alerts, i.e.:

$$GRB_{alerts} \in ToO_{alerts}$$

The following parameters can be defined:

$T_{mission}$	The duration of the operational mission (NoP.)
GRB_{obs}	The per-year total number of successful observations (40 over the duration of the mission; this is the science requirement.)
$GRB_{alerts/year}$	The total number of GRB-alerts (external) received by the ATHENA mission per year.
F_{cand}	The fraction of $GRB_{alerts/year}$ with sufficient x-ray flux 4 hours after receipt of the alert, and sufficiently localised, to perform SG4.1 science.
FoR	The fraction of sky accessible for TYPE_1 (Narrow-field) science observations.
GRB_{valid}	The number of GRB-alerts (external) with sufficient flux 4 hours after receipt, and in the FoR.
F_{accept}	The probability that the Project Scientist will accept the alert (SOC decision point.)
A_{inst}	The probability that the mission is able to pursue the GRB (MOC decision point.)
$GRB_{pursued}$	The number of GRB-alerts that are pursued.
ε_{resp}	The fraction of GRB_{alerts} for which the ATHENA mission is required to observe the GRB_{alert} within 4 hours.

Under the assumption of isotropic distribution of GRB_{alerts} in the sky[1], the following relationship to calculate GRB_{valid} can be stated:

$$GRB_{valid} = T_{mission} \times GRB_{alerts/year} \times F_{cand} \times FoR$$

[1] This allows the geometry of the FoR and the resulting sky coverage throughout the year to be ignored; this is a valid assumption because GRBs are extra-galactic in origin.

The value of $GRB_{pursued}$ can then be determined by considering the SOC and MOC decision points.

$$GRB_{pursued} = GRB_{valid} \times F_{accept} \times A_{inst}$$

Leading to the equation for ε_{resp}.

$$\varepsilon_{resp} = \frac{GRB_{obs}}{GRB_{pursued}}$$

Given that $GRB_{alerts/year}$ and F_{cand} are parameters external to the Mission architecture, and assuming $A_{inst} = 0.85$ and $F_{accept} = 0.98$, the resulting trade-space between FoR, ε_{resp} and NoP duration is shown in the following figure.

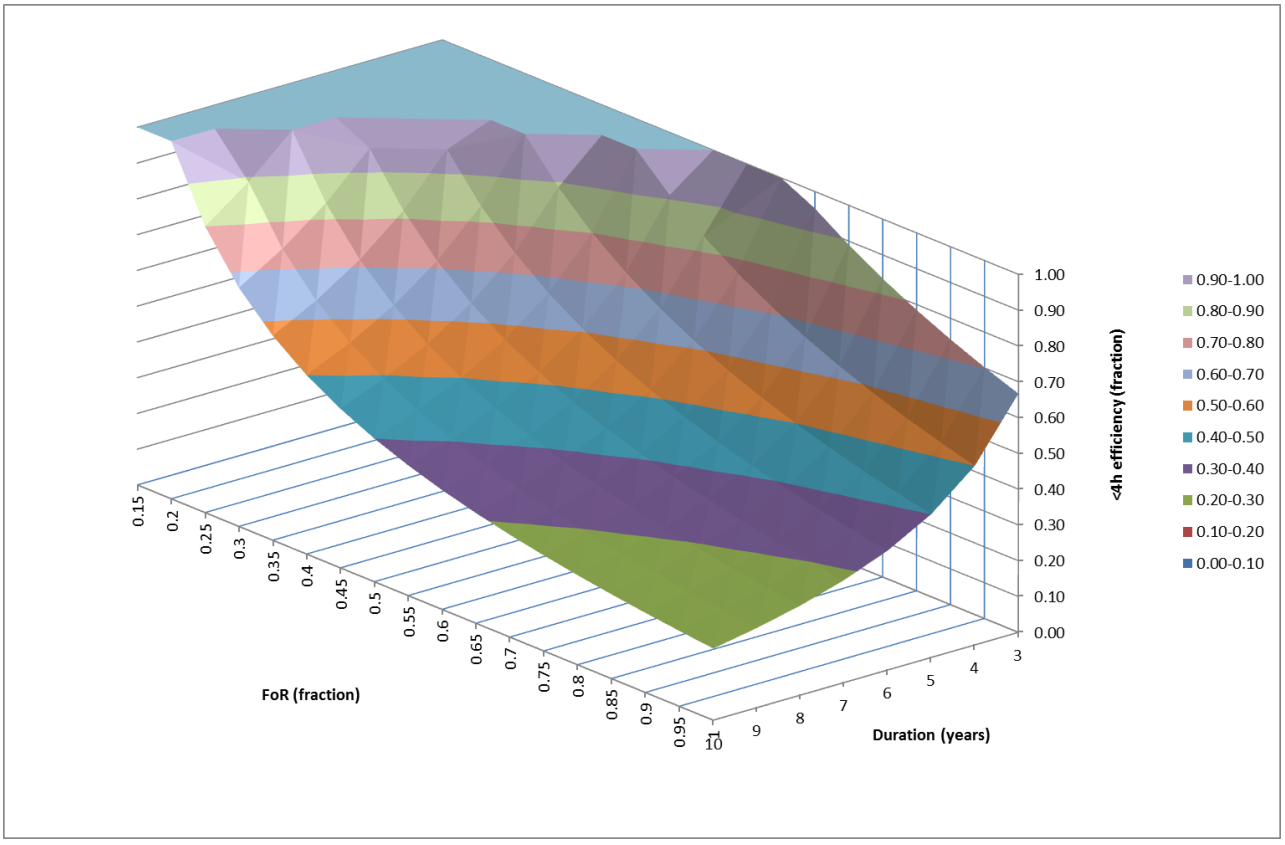

Figure 7: Relationship between FoR, $T_{mission}$ and resulting ε_{resp} in pursuit of the requirement (over the flat-top area the requirement for 40 GRBs over the NoP cannot be met)

Table 7: Relationship between FoR, $T_{mission}$ and resulting ε_{resp} in pursuit of the requirement (1.00 indicates the flat-top area where the requirement for 40 GRBs over the NoP cannot be met.)

FoR [fraction] \ NoP Duration [years]	3	4	5	6	7	8	9	10
1	0.67	0.50	0.40	0.33	0.29	0.25	0.22	0.20
0.95	0.70	0.53	0.42	0.35	0.30	0.26	0.23	0.21
0.9	0.74	0.56	0.44	0.37	0.32	0.28	0.25	0.22
0.85	0.78	0.59	0.47	0.39	0.34	0.29	0.26	0.24
0.8	0.83	0.63	0.50	0.42	0.36	0.31	0.28	0.25
0.75	0.89	0.67	0.53	0.44	0.38	0.33	0.30	0.27
0.7	0.95	0.71	0.57	0.48	0.41	0.36	0.32	0.29
0.65	1.00	0.77	0.62	0.51	0.44	0.38	0.34	0.31
0.6	1.00	0.83	0.67	0.56	0.48	0.42	0.37	0.33
0.55	1.00	0.91	0.73	0.61	0.52	0.45	0.40	0.36
0.5	1.00	1.00	0.80	0.67	0.57	0.50	0.44	0.40
0.45	1.00	1.00	0.89	0.74	0.64	0.56	0.49	0.44
0.4	1.00	1.00	1.00	0.83	0.71	0.63	0.56	0.50
0.35	1.00	1.00	1.00	0.95	0.82	0.71	0.64	0.57
0.3	1.00	1.00	1.00	1.00	0.95	0.83	0.74	0.67
0.25	1.00	1.00	1.00	1.00	1.00	1.00	0.89	0.80
0.2	1.00	1.00	1.00	1.00	1.00	1.00	1.00	1.00
0.15	1.00	1.00	1.00	1.00	1.00	1.00	1.00	1.00

The proposed implementation is a 60% FoR, 5 year NoP (note that in §2.3, the NoP is set to 5 years even though the derivation from the Mock Observing Plan results in 4 years), resulting in $\varepsilon_{resp} = 0.67$ (green in the table above). We can note from the above figure and table that extensions in the operational phase considered, or increases in the FoR, will improve the statistics of captured GRBs considerably, and allow a corresponding relaxation in the response requirement, which will be difficult to meet.

Parameter name	Definition	Quantity	Justification	Comment
<Mission Duration>	Duration in years.	5	From the proposal: ATHENA has a baseline mission lifetime of 5 years, although for such an ambitious mission, consumables should be sized to enable an extension of at least 5 more years. A preliminary mock observation plan has been assembled using typical targets for both the driving science and the observatory science. Considering a conservative observing efficiency of 75%, this shows that ATHENA can reach the science goals of the Hot and Energetic Universe theme during the baseline mission, while preserving a large fraction (30-40%) of the available time for observatory science.	Better justification to come from the core and observatory net observing time requirements. Currently 5 years - information in proposal implies 890 days core science, 479 days observatory (assuming 65/35 split and 75% eff.) If the requirement on 40 GRBs is made a goal can use 10 years here?
<GRB_alerts_year>	All sky total GRB-alerts received by the SGS per year.	200	A pool of 200 GRBs per year, expected from external GRB triggers in the ATHENA era.	Some sort of justification is going to be required, based on expected facilities etc. This number drives the breakdown so is very important. A list of facilities is provided (LOFAR, SKA, ALMA, JWST etc.) which will be the sources of the triggers.
<GRB_alerts_total>	All sky total GRB-alerts received by the SGS over the NoP.	1000	Calculated.	At 50% confidence level (poisson statistics)
<F_cand>	Fraction of <GRB_alerts_total> (i) with sufficient x-ray fluence 4 hours after receipt, and (ii) sufficiently localised to allow SG4.1 science to be conducted.	0.12	From the proposal: Assuming that 12% of the 200 GRBs will have sufficient fluence 4 hours after the trigger.	The assumption is that the validation pre-conditions for F_cand are: (i) the flux of the GRB-event (in detection band) **at the time of receipt** - correlated with the x-ray fluence, otherwise the observatory will need to respond to ~100 ToOs per year assuming 50% FoR. (ii) sufficiently localised (3' to allow acquisition with X-IFU.) This fraction, supplied by the scientists, should also take into account the <time between the external observation and ToO-alert receipt at ESAC>, i.e. the latency in the alert-provider. They won't be able to impose any requirements on the ToO-suppliers, as they are outside the system.

Parameter name	Definition	Quantity	Justification	Comment
<FoR>	Fraction of the sky accessible with the observatory.	0.6	Implementation requirement on mission, derived from above.	Because of the isotropy assumption on GRB-locations, there is no need to specify the geometry of FoR. If we move away from the isotropic assumption, then the geometry of the FoR will need to be taken into account when specifying (i.e. switch to +/- xdeg.) (example: if the locations where always at the poles, then they would always be accessible; alternatively if they were distributed on the circumference of the ecliptic, they would only be accessible 1/3rd of the time.) Note that GS processing of GO observations requirement (25 days) from previous SciRD was linked to the FoR geometry, to allow re-observation if something goes wrong. Don't see this in the proposal yet. Note that there is no apparent reason why anti-sun direction pointing cannot be achieved (giving 75% FoR), but will require rotating solar arrays of course.
<valid_GRB_alerts>	Number of <GRB_alerts_total> (i) with sufficient fluence 4 hours after receipt, and (ii) sufficiently localised to allow SG4.1 science to be conducted, (iii) in FoR.	72	Calculated.	This is the quantity to which 'GRB efficiency' of 40% applies to in the proposal. Assuming isotropic distribution of GRB-locations, this equation is valid for all FoR geometries. A move away from isotropy will affect this number. However, probably one should imagine the source distribution for TOOs is not uniform - (i) depending on what the triggering facility is, and (ii) key measurement is looking at features in the soft X-ray band where galactic absorption may be confusing. THEREFORE it could be that we concentrate on TOOs with galactic latitude > 30 degrees (TBC). My current understanding is that a move away from isotropy will, when combined with the geometry of the FoR, affect the statistics of the ToO being in the FoR. A simple example is that if they always occur at the galactic poles, then they will always be in the FoR. The form of the spatial distribution of ToOs is an output of the SST, and will, when fed through the decomposition, modify the statistics and ultimately the requirement for less than 4 hours for 80% of cases (i.e. may be reduced to 60% of cases or something) - so very important to get a good handle on with the scientists as it may influence the chosen solution significantly.

Parameter name	Definition	Quantity	Justification	Comment
<F_accept>	Fraction of F_cand that are selected for pursuit by PS.	0.98	Some function of the nominal observing plan.	Represents PS decision to not pursue ToO based on current observation importance (i.e. some small % of valid ToO-requests will be refused because the current observation is more important.) Note that this decision is taken w/o any knowledge of the predicted state of the SC (X-IFU). OR IS IT!?!?!? At the moment assume we chase the GRB even though we will not always meet the requirement - ASK the scientists!
<Inst_availability>	Probability that the ATHENA mission is available to pursue the GRB.	0.85	Same as Type#1 observation availability.	This is not the same as the mean operational availability - it is more like the MOC decision point (analogous to the SOC PS decision factor), and will take into account OCMs, calibration campaigns etc., but not for example slewing. This factor may not be included here depending on the fidelity of the simulation. It can also go into the ToO simulation. This factor may include the decision not to proceed if X-IFU is not going to be available in a reasonable timeframe.
<pursuable_GRBs>	Number of <valid_GRB_alerts> that are pursued, i.e. (i) not rejected by PS, (ii) occurring during available periods.	59.976	Calculated.	
ε_resp	Fraction of <pursued_GRBs> for which **the mission** must observe the ToO within 4 hours.	0.67	Implementation requirement on the mission, derived from above.	Named Ground Segment efficiency in proposal - this is wrong because it is a mission requirement (not just GS). This is going to include everything in the chain and is the true requirement to be placed on the ATHENA+ mission.
<SG4.1 observed GRBs>	GRBs, with sufficient fluence 4 hours after the trigger, observed with X-IFU within 4 hours of the trigger.	40	From the proposal: SG4.1 requires 40 distant GRB-afterglow observations.	Science Requirement - this will need to be reduced at some point? Best approach would be to make it a goal (i.e. applicable over NoP+EoP). - 50 for proxy statistics.

Table 8: Budget for GRB efficiency decomposition ([G] FoR case)

6.3 Derived Requirements

The derived requirements are shown in the following figures for the two cases which combine the goals and requirements on FoR and ToO-response, both for a 5 year NoP.

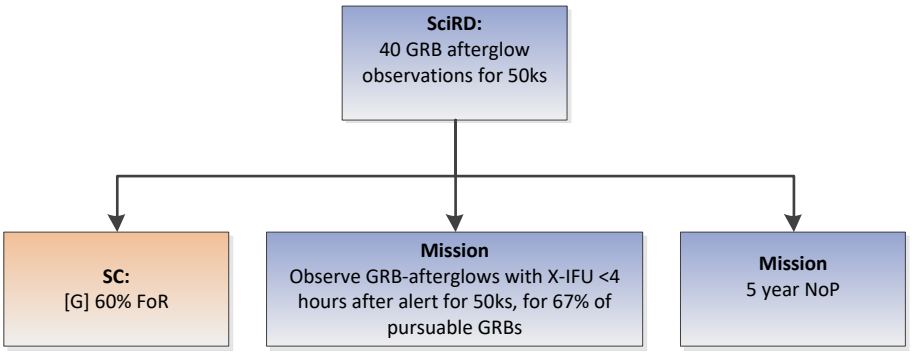

Figure 8: GRB trigger efficiency decomposition ([G] FoR case)

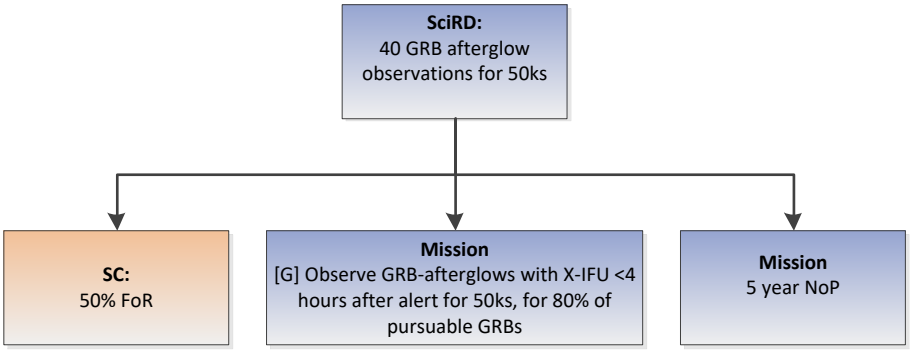

Figure 9: GRB trigger efficiency decomposition ([G] ToO-response case)

Notes:

Note the meaning of 'pursuable'! This is a GRB that meets all the criteria for pursuit; it does not imply that it is pursued (modelling will reveal that some are not reachable within a reasonable time so will not be pursued).

Scheduling constraints could be imposed to improve system-reactivity for a constrained architecture, e.g. synchronise X-IFU nominal observations (cooling cycle) to GS-visibility/availability – but this is a big constraint.

Or schedule OCMs, other interruptions to occur whilst the X-IFU is down (an OCM timescale ~same as cooling cycle down-time), although the benefit will be slight and probably not worth the additional operational complexity.

7 EFFECTIVE AREA & GRASP

Note: Unlike the previous issue of the MBD, the entire Effective Area of the SC is specified to the Prime, which now has control over all terms which contribute to this (Mirror A_eff, SC pointing & misalignment contributions). Note also that the specification for the SC A_eff is now on the telescope LoS, and not at the target as per the previous MRD (i.e. the A_eff loss due to telescope APE is not considered any more).

7.1 MRD Requirements

ID	Requirement
Effective Area - Effective Area - X-IFU Observations	
Note:	*The following requirements correspond to the Overall Effective Area, corresponding to the requirements in the SciRD (i.e. Mirror, PL QE, vignetting all considered).*
R-MIS-230	The ATHENA Mission shall perform X-IFU Observations with a narrow target at the telescope LoS with an overall Effective Area >1.01m^2 at 1 keV.
R-MIS-240	The ATHENA Mission shall perform X-IFU Observations with a narrow target at the telescope LoS with an overall Effective Area of >0.19m^2 at 6 keV.
Effective Area - WFI Observations	
R-MIS-250	The ATHENA Mission shall perform WFI Observations with a narrow target at the telescope LoS with an overall Effective Area >TBD m^2 at 0.2 keV.
R-MIS-250	The ATHENA Mission shall perform WFI Observations with a narrow target at the telescope LoS with an overall Effective Area >1.17m^2 at 1 keV.
R-MIS-260	The ATHENA Mission shall perform WFI Observations with a narrow target at the telescope LoS with an overall Effective Area >0.22m^2 at 6 keV.
R-MIS-270	The ATHENA Mission shall perform Wide Field observations with a grasp of >0.333m2deg2 at 1 keV.
R-MIS-280	The ATHENA Mission shall perform Wide Field observations with a grasp of >0.032 m2deg2 at 6 keV.
Effective Area - Fast observations	
R-MIS-281	The ATHENA Mission shall perform Fast observations with an overall Effective Area at the target of >TBD m^2 at 0.2 keV.
R-MIS-282	The ATHENA Mission shall perform Fast observations with an overall Effective Area at the target of >1.17m^2 at 1 keV.
R-MIS-283	The ATHENA Mission shall perform Fast observations with an overall Effective Area at the target of >0.22m^2 at 6 keV.

7.2 Effective Area Decomposition

7.2.1 Narrow-Field observations

The Effective Area of Narrow-Field observations on the telescope LoS at an x-ray energy e [$A_{eff\_NF}(e)$], is a product of the Effective Area provided to the focal plane by the SC [$A_{eff\_SC}(e)$], and the QE of the X-IFU [$Q_{WFI}(e)$], including all effects at PL-level (detector and filter).

$$A_{eff\_NF}(e) = A_{eff\_SC}(e).Q_{X-IFU}(e)$$

7.2.2 Wide-Field observations

The Effective Area of Wide-Field observations at an x-ray energy e [$A_{eff\_WF}(e)$], is a product of the Effective Area provided to the focal plane by the SC [$A_{eff\_SC}(e)$], a vignetting correction factor [$V(e)$] in the case of the specification of the integrated Effective Area over the Wide-Field FoV, and the QE of the WFI [$Q_{WFI}(e)$], including all effects at instrument-level (detector and filter).

$$A_{eff\_WF}(e) = A_{eff\_SC}(e).V(e).Q_{WFI}(e)$$

The anticipated $A_{eff\_SC}(e)$, of the telescope, assuming perfect on-axis pointing, is shown in Figure 7. The anticipated overall $Q_{WFI}(e)$, with and without a filter in the optical path, is shown in Figure 9. From these requirements at 1 and 6keV have been extracted. For the on-axis response, $V(e) = 1$.

For the Grasp requirements, we multiply the FoV-averaged response by the solid angle FoV of the WFI instrument:

$$G = A_{eff\_WF\_average}(e) \cdot \Omega$$

The anticipated overall $Q(e)$ of the X-IFU/WFI instruments from [RD04] are shown in Figure 10, Figure 11. From these requirements at 1 and 6 keV have been extracted. $P_{SC}(e)$ accounts for the vignetting effects associated with pointing and misalignment of the telescope as described in §5.3.2.

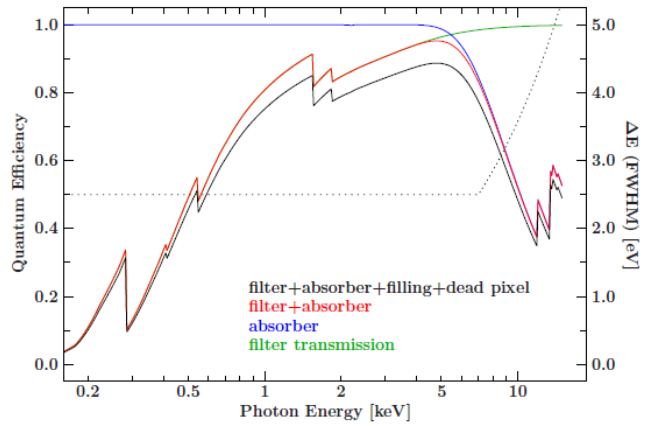

(a) QE of the combination of filter attenuation, filling factor, dead pixel fraction, and absorber efficiency. The plot also displays the energy resolution of the instrument.

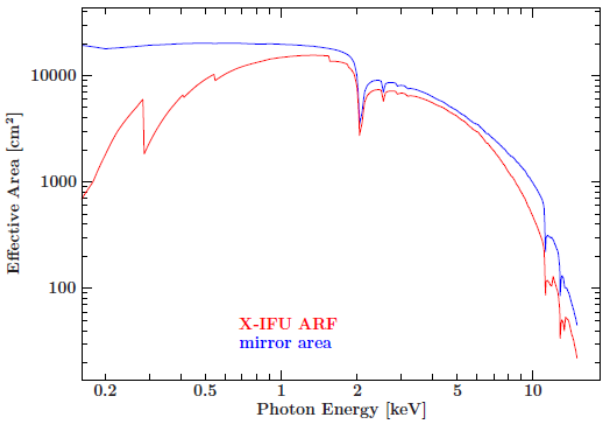

(b) ARF in comparison to the effective area of the telescope.

Figure 10: (a) Anticipated X-IFU QE (black line=overall) and (b) Effective Area as a function of energy compared to the anticipated SC (telescope) Effective Area (nb: for the original large telescope, 2m^2 @ 1 keV)

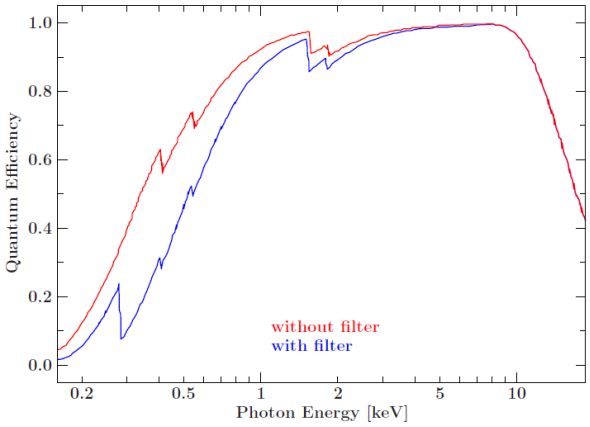

Figure 11: WFI anticipated QE with and without filter as a function of energy

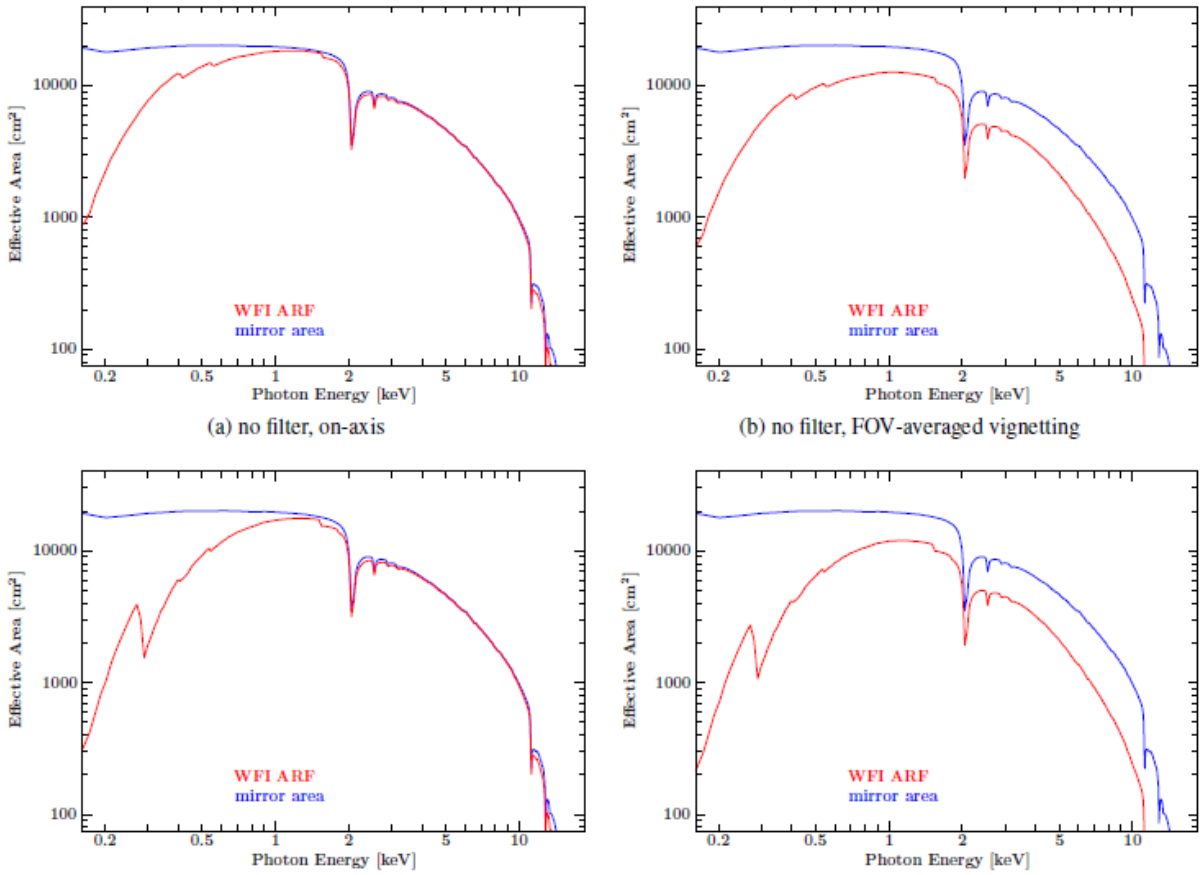

Figure 12: Anticipated Wide-Field on-axis and average Effective Area as a function of energy, with and w/o filter (nb: for the original large telescope, 2m^2 @ 1 keV)

7.2.3 SC Effective Area (Example Decomposition)

The Effective Area provided by the SC is the product of the MA Effective Area on the MA optical axis (including all internal misalignments, contamination etc.), multiplied by a reducing factor to account for the vignetting effects of any global pointing misalignments, i.e.:

$$A_{eff\_SC}(e) = A_{eff\_mirror}(e).P_{SC}(e)$$

7.2.3.1 SC-Level Vignetting Effects

Note: This section outlines the approach used in the CDF study to quantify [$P_{SC}(e)$].

In the CDF we introduced a reducing factor to account for the vignetting effects of any pointing misalignments, [$P_{SC}(e)$], set at <2% at all energies up to 10 keV. Two effects were considered:

- The LoS effective area of the telescope will be modulated (reduced) by any mis-alignment between the telescope LoS and the optical axis of the MA – this will be caused by any relative change in the geometry between the Mirror and the focal plane of the instrument (α)

- Additionally, because the target will not be located precisely on the telescope LoS (APE error - β), an additional vignetting term can be present to further reduce the A_eff at the target itself. *Note: β is no-longer considered in the current specification, which considers only A_eff on the telescope LoS.*

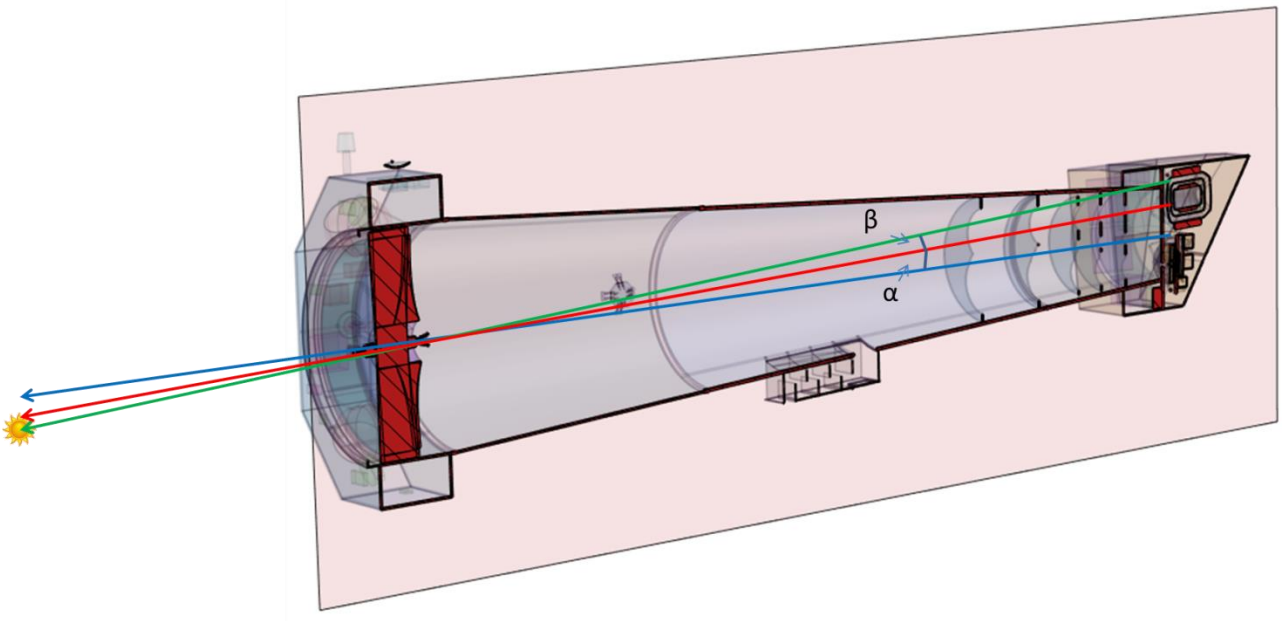

Figure 13: Optical axis (blue) and LoS (red) mi-alignment (σ), and LoS APE (β) will cause vignetting at the target

This variation will have two undesirable effects: A reduction in effective area, and a variation in effective area, which may be important for science related to X-ray timing, and would imply control of the instrument intrinsic effective area variation to a small level compared to the source variation that is being observed (and at the frequencies of interest.)

Figure 14, taken from , shows the vignetting parallel and perpendicular to the reflection plane for a reference telescope design. Figure 15 shows an equivalent vignetting curve calculated using the ESA reference telescope model.

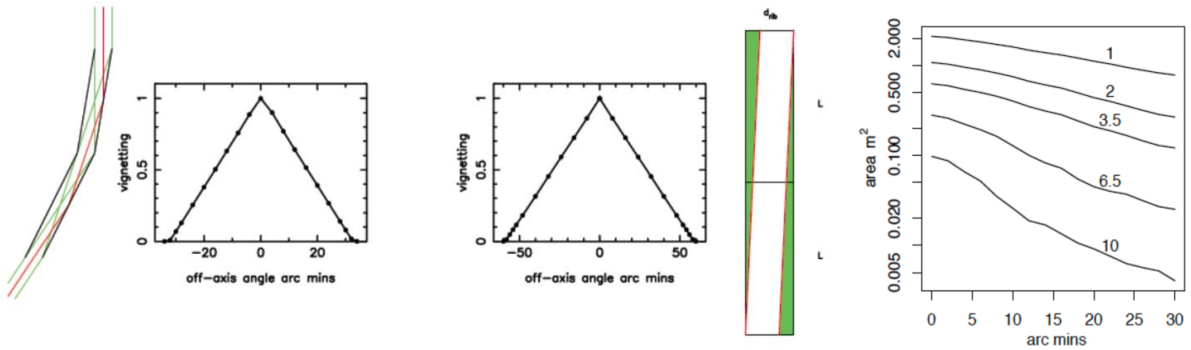

Figure 14: [left, middle] vignetting functions parallel and perpendicular to the reflection plane; [right] effective area loss at various energies as a function of off-axis angle

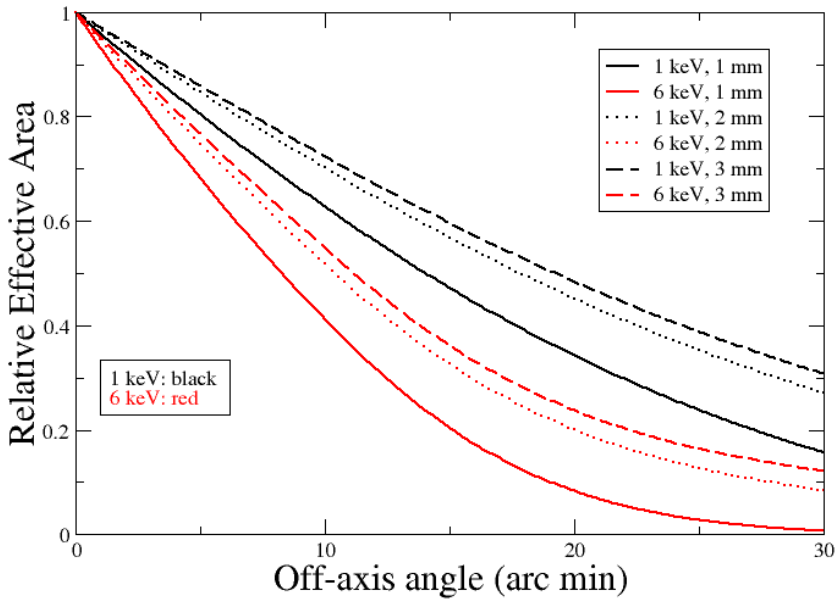

Figure 15: SC vignetting as a function of off-axis angle from the reference telescope model [RD28]

In the CDF, a preliminary requirement was set to restrict the effective area loss at the target due to vignetting to less than 2% at all energies.

Note: this corresponds to an initial calculation for the angle resulting in 1% loss at 10 keV for the reference telescope with 1mm rib-spacing – see Figure 14. The calculation was performed using the reference telescope model 9[RD28], with the following results for the angular error corresponding to 1% effective area loss due to vignetting:

- *1 keV 0.3 arc min= 18"*
- *6 keV 0.2 arc min = 12"*
- *10 keV 0.15 arc min = 9"*

A 20" value was taken, corresponding to 10 keV (the worst-case energy), which for the CDF study was split into a 10" error on the APE between the LoS and Optical Axis of the telescope, and the 10" APE requirement, driven by the WFI Window mode.

A preliminary requirement was set in the CDF study to achieve a knowledge of the variation of Mirror Effective Area at the target to better than 1% of the instantaneous peak response at all energies. This requirement has currently been removed from the baseline requirements (in any case the 2% limit on vignetting loss provides also a knowledge within 2%).

Note: this translated to the 7" AKE requirement between the target and the optical axis in the CDF study, under the assumption that the mirror vignetting function is well characterised.

7.2.3.2 Mirror Effective Area

Note: This section outlines the approach used in the CDF study to quantify [$A_{eff\_mirror}(e)$].

The MA Effective Area is calculated using the Reference Effective Area estimate in [RD28]. The following figure shows the *design* (i.e. assuming no losses) A_eff spectrum of a 15-row mirror for three different rib-pitch values.

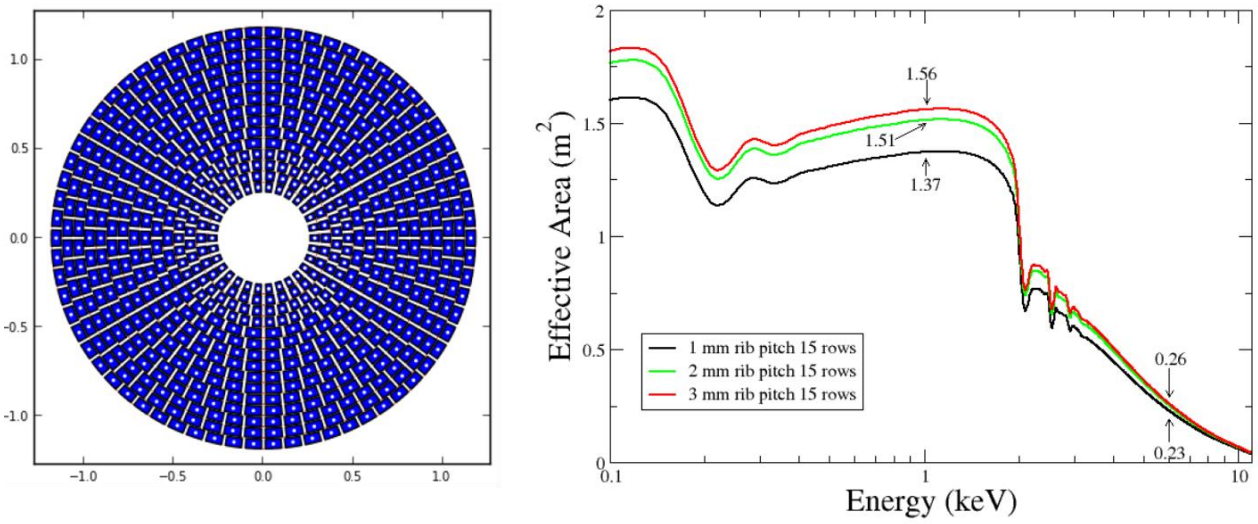

Figure 16: Reference MA layout and A_eff from [RD28]

A number of effects potentially contributing to a reduction of the MA Effective Area were identified in the context of IXO (see table below from [RD40]). To each effect was allocated a reduction in A_{eff} on the basis of preliminary assumptions/analysis.

$$\boldsymbol{A_{eff\_mirror}}(e) = \left(1 - L_{A_{eff_{ext\_obs}}} - L_{A_{eff_{int\_obs}}} - L_{A_{eff_{coat\_imp}}} - L_{A_{eff_{cont\_BoL}}}\right) \cdot \boldsymbol{A_{eff_{design}}}(\boldsymbol{e})$$

Table 9: Mirror effective area reduction budget for IXO

Parameter	Value	Comment	Impact
$L_{A_{eff_{ext\_obs}}}$	0	**External obscuration:** Obscuration induced by elements external, mounted in front of the MM already considered in $\boldsymbol{A_{eff_{design}}}$	τ
$L_{A_{eff_{int\_obs}}}$	0.05	**Internal obscuration:** Misalignment of MM on petal (0.01) Misalignment upp./low. Stack (0.02) Design obscuration factor (0.01) Stack manufacturing error (0.01)	τ $\frac{l_{opt}(f,r)}{l_{plate}}$
$L_{A_{eff_{coat\_imp}}}$	0.01	**Coating imperfections:** uncoated areas, e.g. close to bonding areas/ribs (0.08) coating layer variations, layer thickness and density uniformity (0.02)	$R(E)$
$L_{A_{eff_{cont\_BoL}}}$	0.04	**Contamination effects:** Particulate, based on 100 ppm (BoL) (0.04)	$R(E)$

Molecular, depends on energy, based on <1e-7 gr/cm2 (BoL) (0)

These allocations are in the process of being revisited in the context of ATHENA, considering both optics technology advances and further system (platform) design definition.

7.2.3.2.1 Effect of Contamination

A contaminant is any material in the whole light path of an instrument that should not be there and which affects the efficiency of the instrument. This can be, in the simplest case, frozen water showing-up as oxygen features in spectra, or it might be any other substance that might out-gas from the spacecraft and freeze onto any of the instruments. The two main categories of contamination are particulate contamination, and molecular contamination.

Table 10: Sources of contamination during the different lifecycle phases

Mission Phase	Molecular	Particulate
Fabrication	materials outgassing, machining oils, fingerprints, air fallout	shedding, flaking, metal chips, filings, air fallout, personnel
Assembly & Integration	air fallout, outgassing, personnel, cleaning, solvents, soldering, lubricants, bagging material	air fallout, personnel, soldering, drilling, bagging material, shedding, flaking
Test	air fallout, outgassing, personnel, test facilities, purges	air fallout, personnel, test facilities, purges, shedding, flaking, redistribution
Storage	bagging material, outgassing, purges, containers	bagging material, purges, containers, shedding, flaking
Transport	bagging material, outgassing, purges, containers	bagging material, purges, containers, vibration, shedding, flaking
Launch site	bagging material, air fallout, outgassing, personnel, purges	bagging material, air fallout, personnel, shedding, flaking, checkout activities, other payload activities
Launch/Ascent	outgassing, venting, engines, companion payloads separation maneuvers	vibration and/or redistribution, venting, shedding, flaking
On-orbit	outgassing, UV interactions, atomic oxygen, propulsion	spacecraft cloud, micrometeoroid & debris

	systems	impingement, material erosion, redistribution, shedding, flaking, operational events

Reducing contamination has several implications in the design of ATHENA:

- the optics should have a cover during launch to avoid contamination by particles
- the telescope tube should have low outgassing properties and may need a dedicated cooled outgassing baffle (as for *XMM-Newton*).

7.2.3.2.2 Particulate Contamination

The particulate contamination for IXO has been estimated in [RD39]. Similar results are expected for ATHENA.

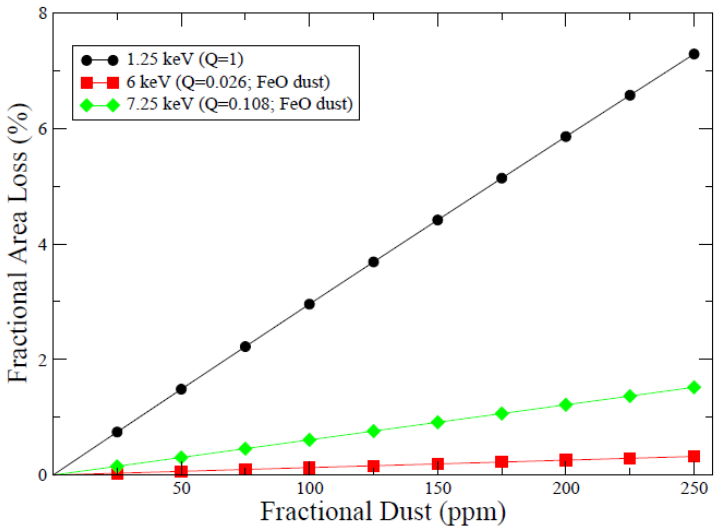

Figure 17: The loss in effective area (expressed as a percentage) as a function of fractional dust contamination for various cases: 1 keV with completely opaque particles (Q=1), 6 keV assuming FeO particles (Q=0.026), and 7.25 keV (just above the Fe K edge) also with FeO particles (Q=0.108). Particulate contamination can be estimated by a simple parametric equation (in the range 0–250 ppm):

$$L_{A_{eff}{}_{particulate\_cont}} = 0.0293 \cdot F_{particulate}(ppm)$$

Where:

- $L_{A_{eff}{}_{particulate\_cont}}$ is the loss in MM effective area due to particulate contamination

- $F_{particulate}(ppm)$ is the fractional level of contamination.

For a design with 125 ppm particulate contamination, the expected loss of effective area can be around 4%.

7.2.3.2.3 Molecular Contamination

Water deposition on the surface of the mirror will not be considered here since the temperature of the mirror surface (around 293 K) is sufficiently high that this is unlikely to contribute significantly. At the moment we apply a limit of <1e-7 g/cm^2.

7.2.3.2.4 Example Budget

The effects discussed previously can be organised into those occurring prior to MM-delivery to the SC, and those occurring thereafter.

Table 11: Example budget split for Effective Area loss

Parameter	Value [fraction]	Comment/reference
Pre-delivery	**0.07**	
Internally-caused obscuration	0.04	
Mis-alignment upper/lower stack	0.02	
Design obscuration factor	0.01	Baffling introduced by the fact that the MM length is sized for the inner most pore
Stack manufacturing error	0.01	
Coating imperfections	0.01	
Uncoated areas, e.g. close to bonding areas/ribs	0.008	
Coating layer variations, layer thickness and density	0.002	
Contamination effects	0.02	
Particulate	0.02	Based on Oesterbroek, 50ppm
Molecular	0	Based on <1e-7 g/cm^2
Post-delivery	**0.03**	
Externally-caused obscuration	0.01	Will drive MM integration rx, ry
External elements, mounted before or after the MMs	0	
Misalignment of the MM onto the MS	0.01	
Contamination effects	0.02	
Particulate	0.02	Based on Oesterbroek, 50ppm
Molecular	0	Based on <1e-7 g/cm^2
Total	**0.1**	

7.3 Derived Requirements

The following figures and table summarise the decomposition of the MRD Effective Area and grasp requirements (all applicable at the beginning of the NoP) into requirements placed on the SC and X-IFU/WFI instruments. Three decompositions are shown:

- Overall effective area for X-IFU observations with narrow field targets at the telescope LoS,
- Overall effective area for WFI observations with narrow field targets at the telescope LoS or fast observations (with WFI fast chip)

- Grasp for WFI observations with wide field targets.

Note 1: All allocations below SC-level are indicated with a dashed line and should be considered as examples of the decomposition to be performed by the Prime.

Note 2: The colours of the boxes indicate the applicability of the requirement. Blue = Mission level (ESA), Green = PL level (PL consortia), Orange = SC level (SC prime) and Pink = MM level (MM provider).

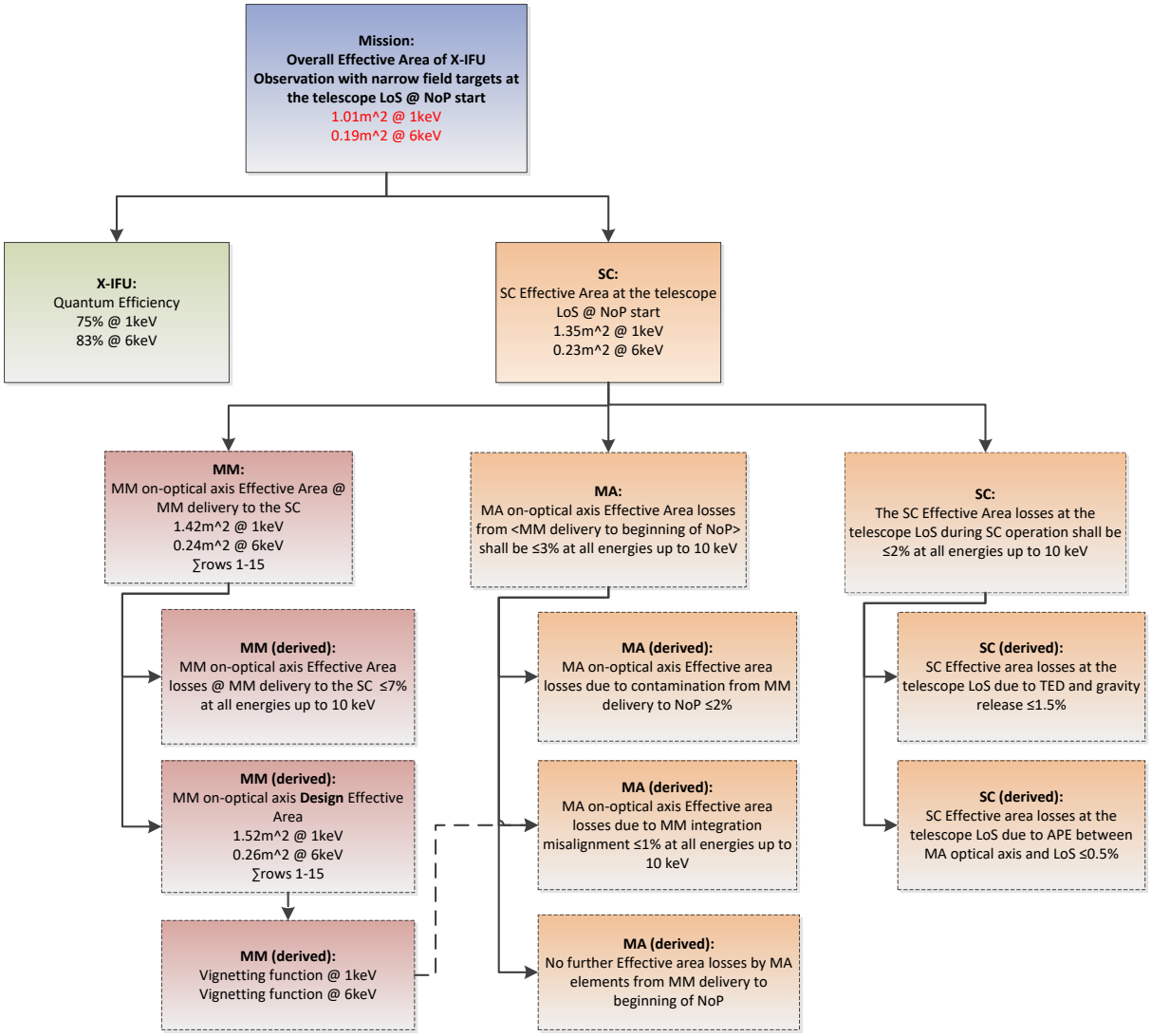

Figure 18: Example summary of the decomposition of the overall effective area for X-IFU observations with narrow field targets at the telescope LoS, assuming the MM A_eff reported in [RD28] for a 1 mm rib-spacing.

Note that the MM vignetting function is derived from the geometries, i.e. changes in the pore geometry such as rib-pitch shall be the driver for the vignetting function, and also for the A_eff. The vignetting function (vs. off axis angle) shall be used to derive the necessary MM alignment accuracy requirements (particularly rotations) during MM integration to achieve the prescribed effective area loss (in the example this value is 1%).

With the MM-layout & reference MM A_eff values as per [RD28] for a 1 mm rib-spacing, and the assumed contamination losses and SC-level losses in the breakdown, the performance at system-level is ~1.35 m^2 @ 1 keV (expected update from the SciRD is 1.4 m^2 TBC). Prospects for increasing the performance beyond 1.4 m^2 are considered to be good, due to:

- Rib-pitch optimisation – [RD28] and the decomposition here assume 1 mm rib-pitch, but current technology developments are considering larger rib-spacings. As shown in Figure 16 this can provide a very significant (10% 1 mm → 2 mm) positive effect on A_eff – this is currently under investigation in the optics technology development
- MM Re-packing exercise – this can provide a ~2-3% positive effect on A_eff as the # of MMs is reduced, see [RD28] – this is currently under investigation in the optics technology development.

As the design work evolves the breakdown will evolve towards budgets at different energies which will give a better granularity on the losses. For instance, the A_eff loss generated by vignetting effects (misalignments) will be more pronounced for higher energies. Conversely, losses due to contamination (particulate) effects will be less severe at higher energies since the opacity of the contaminants is lower at these high energies.

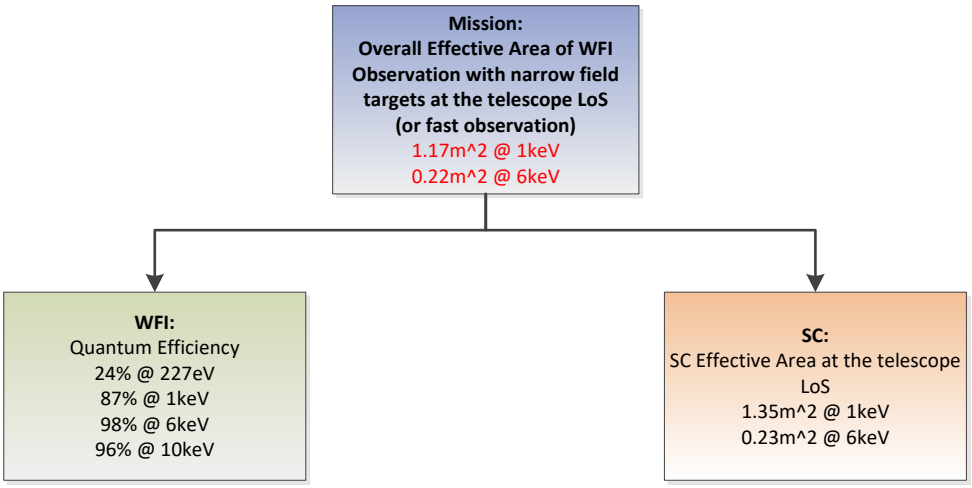

Figure 19: Summary of the decomposition of the overall effective area for WFI observations with narrow field targets at the telescope LoS of fast observations with fast chip. Decomposition of the SC effective area at the telescope LoS is the same as in Figure 18.

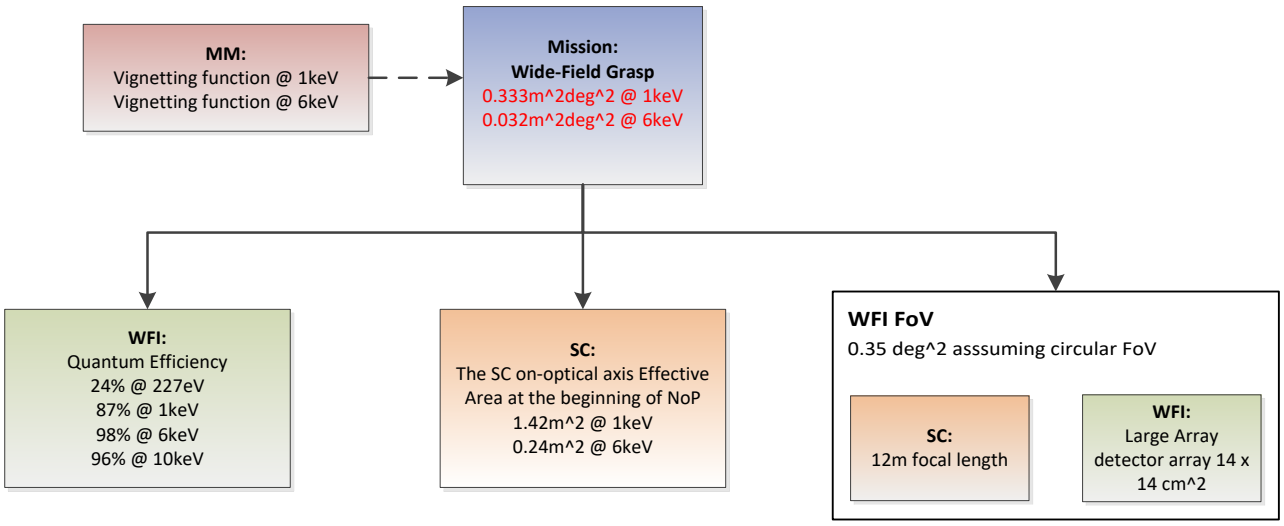

Figure 20: Summary of grasp for WFI observations with wide field targets. Decomposition of the SC on-optical axis effective area at the beginning of NoP is not shown as it is the same as in Figure 18.

Note that the grasp is not flown down to the SRD as it is mainly driven by the MM vignetting function and so largely out of the control of the SC Prime.

Table 12: Summary of values of the effective area requirements expressed in the MRD and SRD according to the decompositions on the previous figures

Energy	On-axis X-IFU A_eff [m^2]	On-axis WFI A_eff [m^2]	Grasp [m^2.deg^2]	MM on-axis A_eff [m^2]	Design MM on-axis A_eff [m^2]	Losses from MM delivery to beginning of NoP	Losses during operation (vignetting factor)	SC on-optical axis A_eff [m^2]	X-IFU QE	WFI QE	WFI FoV [deg^2]	WFI average vignetting factor (average over FoV)	Wide field WFI A_eff (average) [m^2]
1keV	**1.01**	**1.17**	**0.333**	1.42	1.52	0.97	0.98	1.35	0.75	0.87	0.35	0.69	0.95
6keV	**0.19**	**0.22**	**0.032**	0.24	0.26	0.97	0.98	0.23	0.83	0.98	0.35	0.40	0.09

8 FIELD OF VIEW

8.1 MRD Requirement

ID	Requirement
R-MIS-430	The ATHENA Mission shall perform Narrow Field observations with a Field of View of 5' diameter.
R-MIS-440	The ATHENA Mission shall perform Wide Field observations with a Field of View of 40' diameter.
R-MIS-441	The ATHENA Mission shall perform Fast Chip observations with a Field of View of TBD diameter.

8.2 Decomposition

Using the angle of view formula:

$$\alpha = 2atan\left(\frac{d}{2F}\right)$$

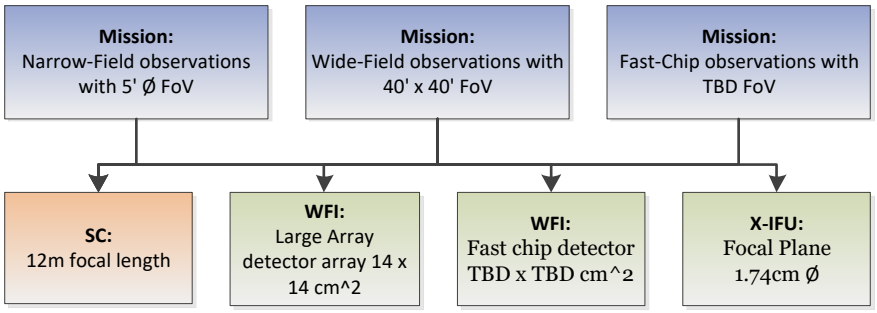

Figure 21: Field of view decomposition

9 TOO REACTION TIME

Note: Please refer to [RD08] for the model which controls this decomposition.

9.1 MRD Requirements

ID	Requirement
ToO Reaction Time	
R-MIS-630	The ATHENA Mission shall be able to perform Narrow field observations of a GRB-ToO ≤4 hours for ≥50 ks (TBC) for ≥67% of pursuable GRB-ToOs.
G-MIS-160	The ATHENA Mission should be able to perform Narrow field observations of a GRB-ToO ≤4 hours for ≥50 ks (TBC) for ≥80% of pursuable GRB-ToOs.
R-MIS-640	The ATHENA Mission shall perform observations of all ToO types ≤12 hours of the receipt of an external ToO alert for ≥95% of pursuable ToOs.

9.2 Decomposition

The requirement on ToO reaction time is understood to consider the time starting from receipt of an un-validated ToO-alert by the SGS, until the subsequent commencement of TYPE_1 (Narrow-Field) observations of the ToO. The main anticipated steps followed in processing the un-validated ToO-alert are defined in [RD08]. The requirement is interpreted as stating that the CDF(*P*) of the bivariate distribution of response and observing times shall meet the required performance, e.g. for the GRB-ToO requirement case:

$$P(T_r \leq 4 \text{ hours}, T_o \geq 50\text{ks}) = 0.67$$

9.3 Derived Requirements

On the basis of the analysis described in [RD08], the GRB-ToO requirement has been decomposed to the following tier-1 items in the Product Tree [RD03] as follows.

With the replacement of Malargue with Kourou as an uplink GS, the allocations for the GRB-ToO requirement are now just sufficient (i.e. the model shows the requirement is met).

Note: depending on the observing plan, # of pointings etc., a faster SC agility may be required to be compliant with the SC availability requirement defined in §3 – this will be derived by the Prime as part of the Operational Availability budget.

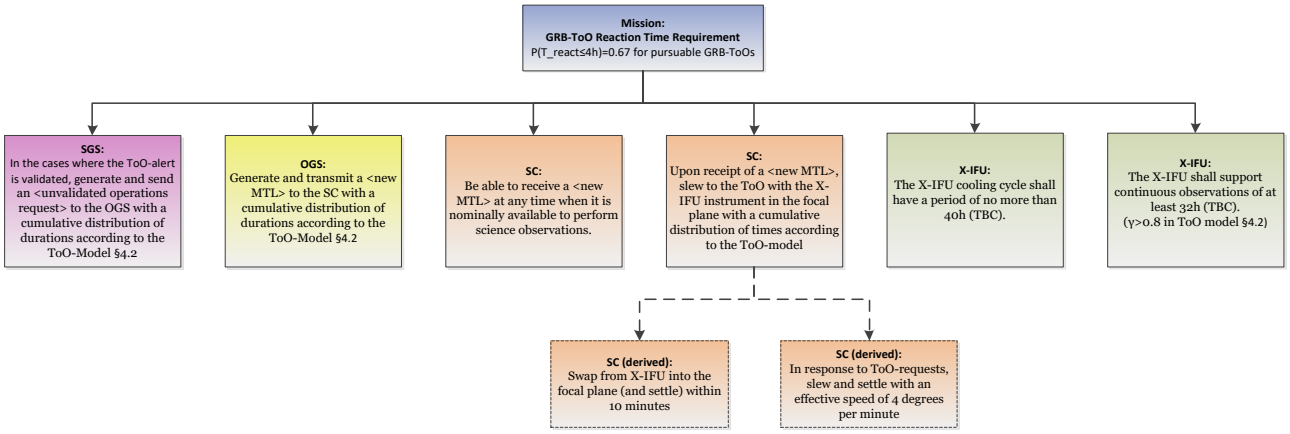

Figure 22: GRB-ToO response time requirement decomposition

10 SCIENCE TELEMETRY LATENCY

10.1 MRD Requirement

ID	Requirement
Latency	
R-MIS-840	The ATHENA Mission shall make available level 1 data to the user for their observation within 15 working days (TBC) of the end of the observation.
R-MIS-850	The ATHENA Mission shall make available Quick Look data (TBC) to the user for observations which were a ToO within 2 working days (TBC) of the end of the observation.
R-MIS-860	The ATHENA Mission shall make available relevant instrument data to the instrument teams for health checking within 1 working day (TBC).

10.2 Decomposition

The requirements on latency are divided among the PL, SC, OGS and SGS.

10.3 Derived Requirements

The latency requirements have been broken to the following tier-1 items in the Product Tree [RD03].

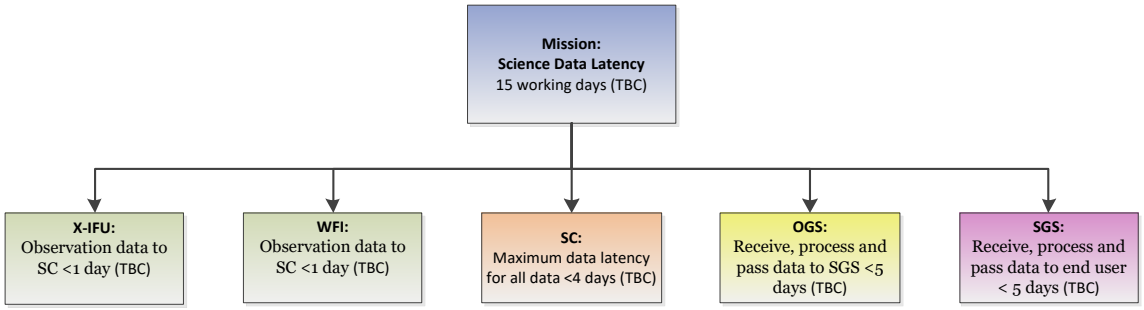

Figure 23: Science data latency requirement decomposition

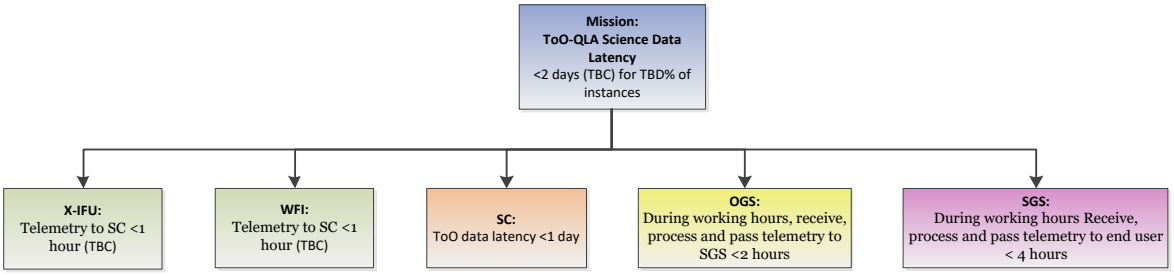

Figure 24: ToO-QLA science data latency requirement decomposition

11 ABSOLUTE TIME ACCURACY

11.1 MRD Requirement

ID	Requirement
R-MIS-470	The ATHENA Mission shall perform all observations with an absolute photon timing accuracy of ≤50 μs.

11.2 Decomposition

The proposed scheme described is derived from experience of the Integral and XMM-Newton satellites, as described in [RD15], [RD16], [RD17].

11.3 Overview

Time correlation is the process of accurately establishing the relationship between a local time system and a reference time system in order to allow the unequivocal referencing of event arrival times. On a satellite observatory the local time system is commonly known as on-board time (OBT) and the global reference system is the Universal Time Co-ordinated (UTC). All events occurring on-board must be referenced to the OBT time system. The OBT local time system is typically maintained by a crystal oscillator (of TBD MHz) located in a Central Data Management Unit (CDMU).

The OBT is initialised at CDMU switch on and continues to run freely from that point. To ensure oscillator stability, the oscillator temperature is normally maintained above local ambient temperature with a constant heat supply, while feedback control of the oscillator environment or frequency might also be enabled. The OBT can be coordinated between on-board subsystems by the CDMU by means of a periodic broadcast pulse on the SC data bus, typically at 1 second period.

All other spacecraft subsystems then may maintain a local copy of the OBT and use this information for timing of internal events. Subsystems will be required to have their local copy synchronised to the CDMU OBT when they are switched on and to maintain synchronisation through the broadcast pulses. CCSDS standards apply to time codes and typically define the word lengths for seconds and fractions of seconds.

11.4 XMM-Newton Experience

In the case of XMM-Newton a packetized telemetry stream is operated, where packets from the various subsystems are encapsulated by the CDMU in frames of fixed size. The instant of transmission of the first bit of every 16th frame was time stamped on board in the local OBT system, by means of a hardware mechanism that latched and stored on-board the OBT at the right moment.

Each GS operates in UTC and is synchronised through a combination of a local oscillator and a GPS clock. On the ground the GS adds an Earth Received Time stamp (ERT, in the UTC reference system) to the first bit of each frame it receives. As the time between the transmission and the reception of the frame is known within a certain accuracy it is possible to correlate the occurrence of the two specific events in the two time references systems. To

correlate the OBT to UTC it is sufficient to subtract from the ERT the signal travel time from the satellite to the GS. This time of flight is calculated in real-time by the mission control system at ESOC from knowledge of the predicted orbital position and the GS location.

Additionally the CDMU and GS timing systems are not infinitely fast and therefore fixed offsets and delays from these components are also considered, based on calibrations made on-ground. To obtain UTC for any OBT it is necessary to fit the pairs of OBT/UTC with a function and use this function to derive the UTC. If there are variations in the OBT oscillator frequency a non-linear fit is required to achieve accurate timing conversion from OBT to UTC over the period of a typical observation.

The XMM Mission Control System (MCS) uses orbit prediction to calculate the signal travel time from SC to GS. This file, which is distributed with the ODF, is currently updated every revolution shortly after perigee and thus represents a very good prediction of the forthcoming orbit. The ODF also includes an orbit file that is produced after completion of the relevant revolution and is known as the reconstructed orbit file because the data are reconstructed from the continuous ranging measurements that are made from the GS to the SC throughout the revolution. The difference in the time correlation products as calculated from the orbit prediction are generally the same as those from the reconstructed orbit file, to an accuracy of 30μs [RD18]. It should be noted that following any anomaly, for example Emergency Safe Attitude Mode (ESAM), there may have been unforeseen changes to the orbit that reduce the accuracy of the prediction. Therefore, observers must use the reconstructed orbit file for their final analysis.

The SC position is measured by a differential correction technique involving an orbital model that takes into account the Earth potential, the gravitational effects of the Sun and of the Moon, the effect of the Solar radiation pressure, and the momentum control manoeuvre data. This model is constrained with ranging and Doppler measurement data providing line of sight position and velocity that are regularly collected when the satellite is visible over the ground station. The accuracy for orbit reconstruction for the eccentric orbit is normally better than 10 meters along the line of sight.

The relationship between OBT and UTC is not linear, as the crystal oscillator is susceptible to ageing and drift. Over time it has been possible to accurately measure the oscillator performance on both short and long time scales.

11.5 INTEGRAL Experience

The *INTEGRAL* data analysis uses essentially three time systems:

1. The Earth Reception Time (ERT), expressed in coordinated Universal Time (UTC), is defined at the reception of every telemetry frame by the GS. The ERT is determined by atomic clocks located within each of the ground stations used by the mission. The ground stations are synchronized using the GPS.
2. The Terrestrial Time (TT) is used to time tag, on-ground, products and physical events recorded within the instruments. The terrestrial time follows precisely the Atomic International Time (TAI) and does not suffer from leap seconds. In the data products terrestrial times are always formatted as double precision real in unit of *INTEGRAL*

Julian Date (IJD), defined as the number of days since the 1st of January 2000 at 0h 0m 0s (TT) (IJD=JD−2451544.5).

3. The On Board Time (OBT) is defined by counting the number of pulses of an oscillator on board the spacecraft. All on board times are represented as 64 bit integers with a unit of 2^{-20} OBT second even if they are less precise in the telemetry.

The *INTEGRAL* time correlation is the relation between IJD and the OBT. It is derived from measurements, in OBT, of the time at which specific telemetry frames leave the spacecraft (more specifically the leading edge of the first frame bit). OBT measurements are then correlated to the ERT of the corresponding frames. Corrections for on board delays, delays within each of the ground stations and light travel time are taken into account.

The on board delays were calculated and calibrated on ground. Unfortunately, at the beginning of the mission, the on board delay was taken into account with a wrong sign in the time correlation software with the net effect that any IJD derived from an OBT had to be corrected by a positive offset.

The delays between the actual event times and the instrument OBT time tags were measured on ground before the launch. These delays were also derived from flight data using contemporary *INTEGRAL* and *RXTE* observations of the Crab pulsar [RD19]. For all *INTEGRAL* instruments and *RXTE*, the differences in arrival times of the first (main) Crab peak in the pulse profile in radio and X-rays have been measured. The differences between the *INTEGRAL* and *RXTE* measurements, (both using the same ground station), of the X-ray - radio delay is a measure of the instrumental delays, taking *RXTE* as the standard. For *RXTE* an X-ray - radio delay of 268 ± 30 μsec was determined.

11.6 Crab calibration

Calibration of absolute timing has concentrated primarily on the Crab pulsar (PSR B0531+21) because radio ephemerides are provided monthly by the Jodrell Bank Observatory. However, the reference to radio timing limits us to the accuracy of the radio ephemerides. The Crab has been one of the best-studied objects in the sky and it remains one of the brightest X-ray sources regularly observed.

As a standard candle for instrument calibration, the 33ms Crab pulsar has been repeatedly studied (monitored) by many astronomy missions in almost every energy band of the electromagnetic spectrum. In the X-ray regime its pulse profile exhibits a double-peaked structure with a phase separation of 0.4 between the first (main) and the second peak. Measurements of X-ray to radio delays between the arrival times of the main pulse in each energy range of the Crab pulsar have been reported using all high-energy instruments on-board INTEGRAL [RD19] and RXTE [RD20]. The time delays were determined to be 280 ±40 μs and 344 ±40 μs, respectively.

The relative timing accuracy may be defined as the difference between the period measured with the X-ray observatory and the period measured at radio wavelengths evaluated at the epoch of the X-ray observations.

The period of the Crab pulsar in X-rays is typically determined using the publicly available epoch-folding software XRONOS. The closest available Jodrell Bank Monthly radio ephemeris [RD21] before and after the X-ray observation are used to interpolate the radio

period P for the time of the first X-ray event of the X-ray observation and the interpolated radio periods used as an initial trial value for the epoch folding. The period derivative $P^{\prime}$ provided by Jodrell Bank needs to be taken into account when folding the X-ray data.

The ephemeris (epoch, P, $P^{\prime}$, $P^{\prime\prime}$) of the nearest radio observation from the Jodrell Bank can be used as a reference to obtain the phase shift between the time of arrival of the main peak in the X-ray profile and the time of arrival of the main peak in the radio profile to give the *absolute* timing accuracy, via the phase shift multiplied by the corresponding X-ray period found during the relative timing analysis, The Crab pulsar shows a shift of –300μs between the peak of the first X-ray pulse with respect to the radio in the results of various missions. Differences in the shifts observed over several decades in energy are marginal with an average value. Error bars quoted for the different X-ray missions have included systematic errors from the radio measurements.

The origin of the electromagnetic radiation emitted from pulsars is still unclear. Several models have been proposed to explain the origin of the high-energy radiation based on different regions of acceleration in the pulsar magnetosphere, such as the polar cap, the slot gap, and the outer gap models. The radio emission model is an empirical one and the radiation is usually assumed to come from a core beam centred on the magnetic axis and one or more hollow cones surrounding the core The estimated average delay between the emission from differing wavelengths is therefore significant and the site of radio production is distinctly different from that of the X-ray emission. The time delay of about 300μs most naturally implies that emission regions differ in position by about 90 km between radio and X-rays energy bands in a simplistic geometrical model - neglecting any relativistic effects - with the radio emitted from closer to the surface of the neutron star. By implication the delay for a given X-ray energy band depends on average distance of region producing the bulk of photons in that band.

Scatter due to uncertainties in the time correlation process may eventually dominate over measurement of the phase of the main peak which by centroiding can be measured with an accuracy of ~μs.

11.7 Additional Considerations for ATHENA

While the XMM-Newton and INTEGRAL experience indicates the required ATHENA timing accuracy should be attainable, it should be borne in mind there are significant differences in ATHENA implementation to be considered:

- Orbit – L2 at a radial distance ~1.5 10^6 km compared with a HEO orbit of ~10^4 to 10^5 km, implying perturbations and their timescales will be very different, and the greater distance will impact ranging capability
- Use of telemetry packets scheme may be modified by latest CCDS standards, CFTP transmission etc., and the adoption of on-board data distribution techniques (*Spacewire*) ‘may render the current approaches obsolete (but hopefully improved)
- Ground contact is not anticipated to be continuous, therefore a daily contact period (e.g. ~3 hours) must be assessed for ranging capability, orbit reconstruction accuracy and propagation etc. Additionally, the nominal use of a single ground station must be examined for potential systematic errors using a single reference time system for ERT.

If anticipated interpolation of ranging would lead to excessive uncertainty, then additional ranging activities will have to be considered as part of operations

- ToO and other observational programmes may require specific timing capability. Also the disruption in planning sequences, pointing modifications etc. would affect the predicted orbital elements and possibly the subsequent data analysis (*especially the QLA*), unless the ranging and time referencing activities also were re-planned and updated.

11.7.1 Error Distribution

Upper limits for the time allocation processes can be estimated, for example using the values reported by [RD15]. They estimated the following:

- The SC clock error to be ~11 μs: Revisit how the ATHENA clock can be improved
- The uncertainty in ground-station delays to be ~5 μs: Revisit with ESOC based on set of GS to be used in 2028
- The interpolation errors to be ~10 μs: Review the effect of more sparse data set
- The error between latching observing time and the start of frame transmission as ~9 μs: Review the OBDH concept for ATHENA
- The uncertainties in the spacecraft orbit ephemeris to be ~30 μs: Check with ESOC what has been achieved with Herschel and GAIA

All these error sources will be random. The resulting scatter can then be considered to be the minimum significant time separation between two arrival times to be considered independent.

11.8 Proposed ATHENA error decomposition

Total PL error	**5 μs**
SC Maximum drift in OBT between consecutive correlation references	5 μs
SC Maximum error in OBT distribution to instrument subsystems	5 μs
SC Maximum error in copying OBT to data transmission	5 μs
Total SC error	**15μs**
OGS Maximum error due to orbital uncertainties (1.5 km)	5 μs
OGS Maximum uncertainty in ground station delay	5 μs
Total OGS Error	**10μs**
SGS Maximum interpolation errors	20 μs
Total SGS error	**20μs**
Total Absolute Time Accuracy (additive)	50 μs

11.9 Derived Requirements

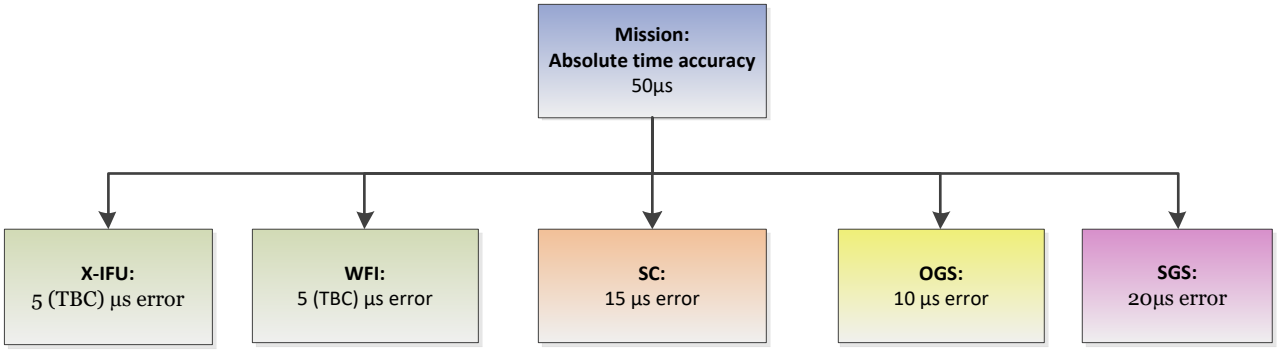

Figure 25: Absolute time accuracy requirement decomposition

12 BACKGROUND

Note: It is anticipated that the Background Working Group will be responsible for this decomposition, relying on simulations performed using the tool developed under the AREMBES activity [C204-110EE].

12.1 MRD Requirement

ID	Requirement
R-MIS-590	The ATHENA Mission shall achieve a non-X-ray background for Wide-Field observations of < 5 10^-3 counts .s^-1 . Cm^-2. keV^-1 (TBC).
R-MIS-591	The ATHENA Mission shall achieve a non-X-ray background for Fast Chip observations of < TBD counts .s^-1 . Cm^-2. keV^-1 (TBC).
R-MIS-600	The ATHENA Mission shall achieve a non-X-ray background for Narrow-Field observations of < 3 10^-4 counts .s^-1 . Cm^-2. keV^-1.

12.2 Decomposition

Note: The justification for this breakdown is TBW. The proposed values are ambitious and will need detailed simulations to confirm their feasibility. The presented decomposition may not be optimal and a higher optical background can be compensated by a lower background for another component.

The MRD requirements are decomposed as in the following figure.

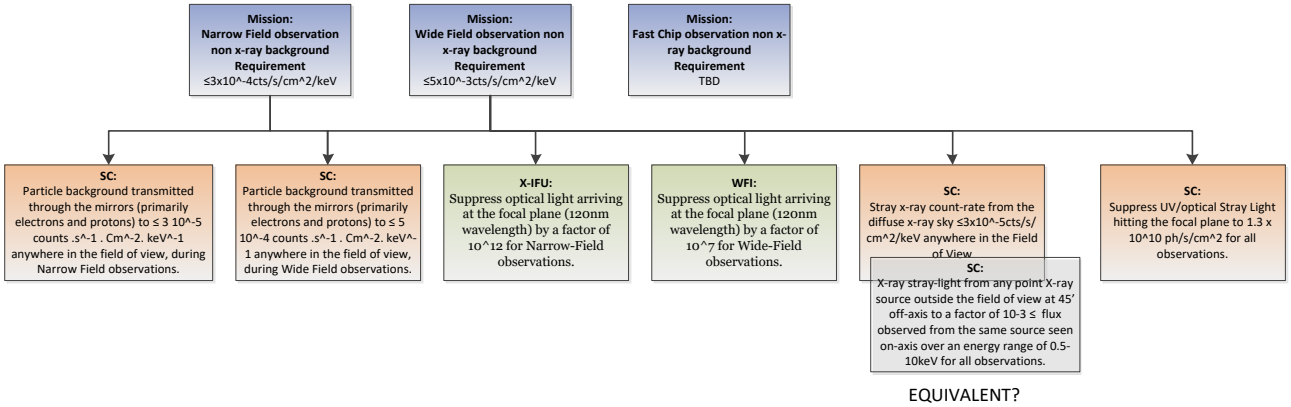

Figure 26: Background requirement decomposition

13 SC (TELESCOPE) POINTING

13.1 Motivation

Note: This section provides an initial definition of the pointing requirements for the ATHENA SC, based on a review of documentation from previous study phases for IXO and ATHENA_L1, and work done during the CDF study (Phase 0) to develop understanding of the requirements, in coordination with the ASST.

Note: All pointing requirements currently to 95 % CL using a temporal statistical interpretation.

Note: It is anticipated that the RPE and possibly APE requirements will be removed in due course from this document and placed in the SC Prime top-level budget document.

13.2 Definitions

These requirements are all applicable to the SC (telescope LoS) in an inertial (e.g. J2000) reference frame. To define the telescope LoS we make use of the following definitions:

MA nodal point: The geometric location in the Mirror Assembly which has the property that rotations around it, to first order, lead to no image motion in the focal plane. The nodal point is located on the optical axis of the MA, on the plane defined by the virtual intersection of the primary and secondary mirrors of the MMs.

Telescope LoS: The telescope LoS is the vector connecting the central pixel of the detector in the focal plane with the MA nodal point.

13.3 Absolute Knowledge Error (AKE)

13.3.1 MRD Requirement

ID	Requirement
Astrometry	
R-MIS-620	The ATHENA Mission shall achieve a reconstructed Astrometric error of <2" to 95% confidence level (TBC) for all observations.
G-MIS-150	The ATHENA Mission should achieve a reconstructed Astrometric error of <0.64" to 95% confidence level for Wide-Field observations.

13.3.2 Decomposition

Note: this has tightened as a result of the analysis presented in [RD44].

This is the astrometry requirement for the a posteriori knowledge of the angular position of an observed object in the sky, and is currently flown directly to the SC (i.e. applicable on-board).

Note: This was relaxed by the ASST from 1" AKE since this is difficult to achieve, particularly with the X-IFU where the improvement from ground-based processing is less (than the factor 3-4 realised by XMM Newton) due to the lack of multiple stars in the image.

Taking the centroid of the primary stellar source may allow some improvements to the AKE, but this is yet to be quantified.

13.3.3 Derived Requirements

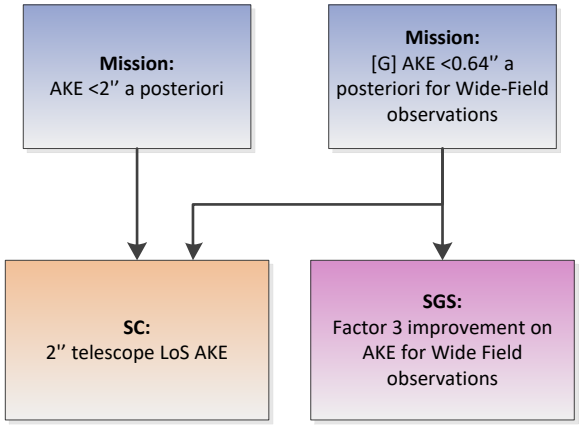

Figure 27: AKE decomposition

13.4 Absolute Performance Error (APE)

13.4.1 SciRD/ConOps Requirement

Window Mode of the WFI instrument.

13.4.2 Decomposition

13.4.2.1 Historical

Note: The following justification is taken from [RD22] and is derived from the need to ensure the target is in the (smallest) FoV instrument. Conversely, for ATHENA_L1 [RD23] the operation of WFI in 'Window Mode' and the simultaneous observation with XMS resulted in an APE requirement of 10" (but this is no longer applicable because there are now no simultaneous observations foreseen.)

For the IXO mission, the requirement for the position of a nominal (boresight) target in the focal plane was needed to ensure that the target was in the FoV of the smallest focal plane instrument, leading to the following requirement:

R-520-10: During any observation with any focal plane instrument, other than the grating spectrometer, the centre of an imaginary point source at the nominal pointing position on the sky shall be maintained within 1mm from the centre of the instrument field of view.

At that time the focal length of the telescope was 20m, equivalent to a 10" pointing offset. An APE requirement of 10" @95% confidence was derived from this mission requirement for transverse x, y axes. The APE requirement around z-axis was TBD but will be much more relaxed. For the envisaged 12m FL of ATHENA, the transverse requirements relax significantly to 17". This is small compared to the FoV of X-IFU (5' in diameter), which is required to be compatible with a typical GRB-location specification accuracy of 3' [RD26].

13.4.2.2 Current

The WFI Fast-Chip Window Mode (high count-rate mode), when the PSF must be located within the WFI window (dimensions of 35 x 35") imposes a limit on the APE. An initial analysis, for a PSF radius of 7" at 95% energy (long tails) at highest energy 10 keV. With 10" APE (includes MPE and RPE, i.e. all frequencies of errors including zero Hz) the worst case would have the PSF edge 17" off centre (just fitting in to the WFI 35/2=17.5" window).

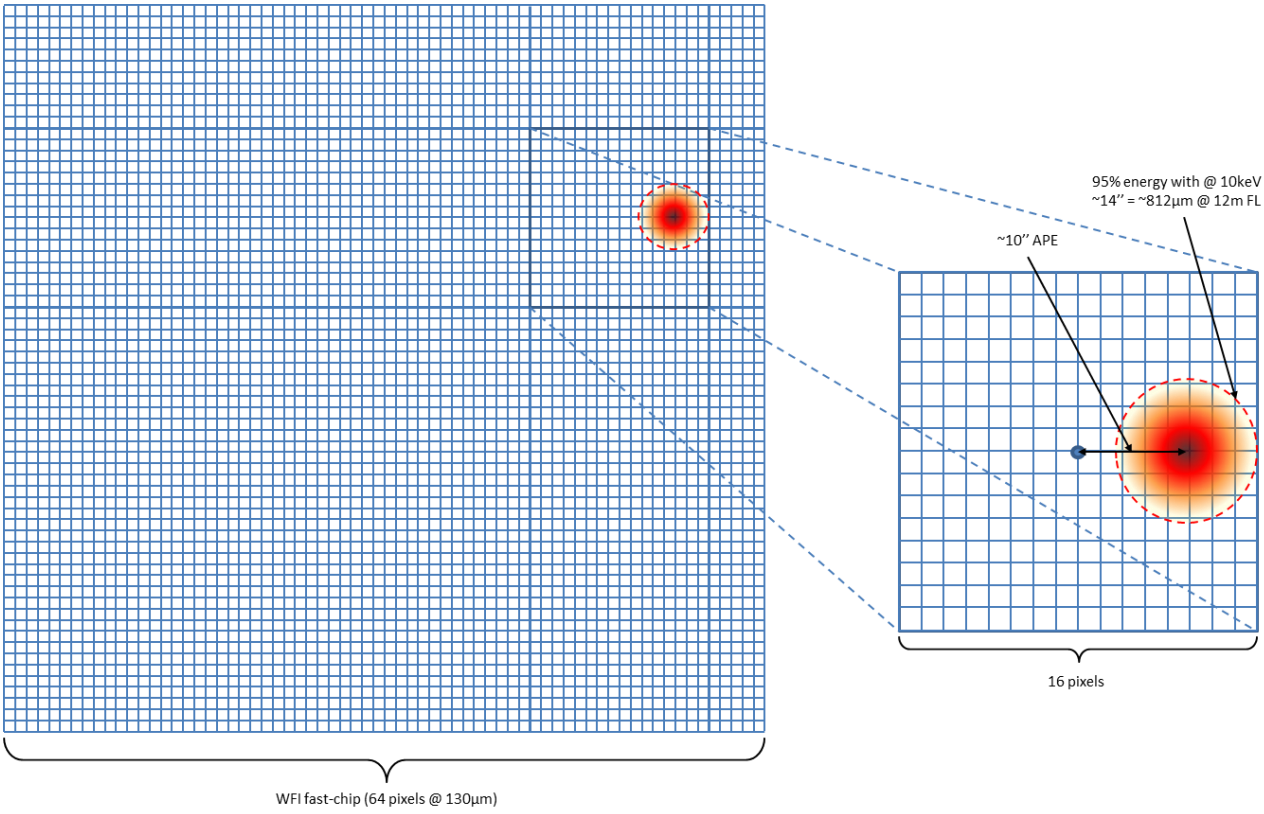

Figure 28: APE requirement driven by WFI window mode

Note: Telescope APE will also be constrained by the <2% cap on Effective Area loss at the target, described in §5.3.2. Whether this requirement will result in an APE tighter than the 10" required by the WFI Window mode will be at the discretion of the Contractor.

A preliminary loose specification of 1' aLoS is made.

Furthermore, a 3" goal APE is an ATHENA L2 update from the scientists based on simulations, but currently has no parent requirement or documented justification. There are the following possible drivers:

- X-IFU fast-sensor array in centre of detector (7" heard in discussion, nothing provided by Consortium)
- WFI FD PSF positioning – no information provided by the Consortium.

13.4.3 Derived Requirements

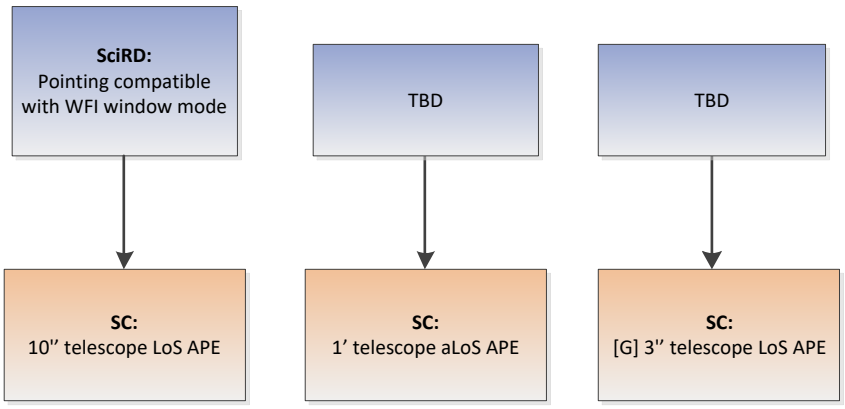

Figure 29: WFI Window Mode Decomposition to APE

13.5 Pointing Drift Error (PDE)

13.5.1 ConOps Requirement

It is envisaged that ATHENA shall be able to perform dithering to disentangle detector effects from true features in the observed objects. Typical long observations, used to observe weak sources, will be split into different pointings. As a minimum a Raster scan with 9 observations centred on the target under observation and separated by 3 pixels is anticipated.

The Raster Mode of Pointing shall be an optional mode for pointing to be used for any observation of duration longer than T_long seconds (T_long shall be a configurable parameter and typically >30ks.) The mode shall comprise a series of exposures of equal duration (T_exp) separated by small slews in order that the telescope axis moves in a raster pattern centered around a given sky direction. The raster coverage shall comprise N lines each of M pointings, with d the angular distance between successive lines and successive steps within one line. N, M and d shall be configurable parameters. The typical Values are M=N=3 and d = 13" (3 x pixels). T_exp is expected to be ~2.5ks under the current assumption for the time taken to move between raster pointings. Then T_long ~ N*M*T_exp.

13.5.2 Decomposition

Note: the following justification is taken from the ATHENA_L1 documentation [RD23] and is derived from the need to remove detector effects. Conversely, the IXO PDE derivation in [RD22] specifies that the PDE is driven by the requirement to minimise the reduction in the effective area of the Raster image. The true requirement needs to be established.

Flows from 3 pixel spacing number above. If a previous raster-point hold encountered a 4" drift to the left, and the current raster point also drifts 4" to the right, there is still no overlap in the 5" diameter HEW due to 3 pixels (13") spacing of points (4+4+5=13).

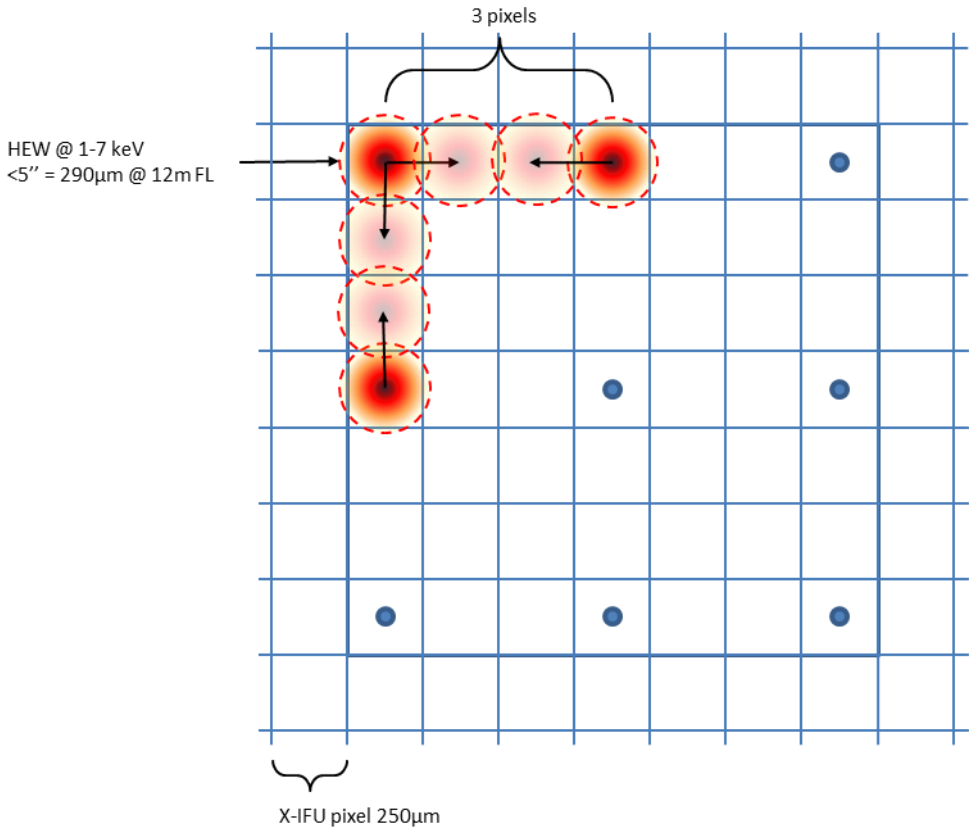

Figure 30: PDE requirement driven by X-IFU reference raster scan

13.5.3 Derived Requirements

A PDE of 4" x, y over the typical exposure time (T_exp=2.5ks) is therefore defined for the 3x3 Raster scan case described above. Longer exposures up to the 100ks requirement are assumed to be split into larger (larger values of N and M) or repeated scans such that the associated duration is unchanged.

Note: if the step size between nominal scan locations is enlarged, the requirement becomes looser.

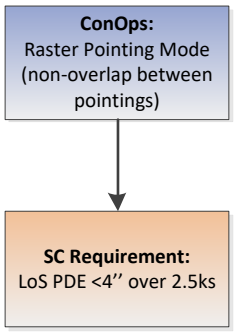

Figure 31: Raster Pointing Mode decomposition to PDE

13.6 HEW Budget (RKE)

13.6.1 MRD Requirements

ID	Requirement
Angular Resolution	
R-MIS-320	The ATHENA Mission shall perform Narrow Field observations with a Point Spread Function (PSF) having ≤TBD" Half Energy Width (HEW) at the target, over an energy range of 0.1 - 6keV.
R-MIS-321	The ATHENA Mission shall perform Wide Field observations with a Point Spread Function (PSF) having ≤TBD" Half Energy Width (HEW) at the target, over an energy range of 0.1 - 6keV.
R-MIS-322	The ATHENA Mission shall perform Fast observations with a Point Spread Function (PSF) having ≤TBD" Half Energy Width (HEW) at the target, over an energy range of 0.1 - 6keV.
G-MIS-330	The ATHENA Mission should perform all observations with a Point Spread Function (PSF) having ≤3" HEW at the target, over an energy range of 0.1 - 6keV.
R-MIS-340	The ATHENA Mission shall perform all observations with a Point Spread Function (PSF) having ≤20" HEW at the target, over the energy range 6 - 15 keV.
R-MIS-350	The ATHENA Mission shall perform all observations, at 25' off-axis, with a Point Spread Function (PSF) having ≤10" HEW, over the energy range 0.1-6keV.

The HEW requirements are all intended 'on ground' i.e. after best knowledge correction of the direction from which the photons were received. Note that without any attitude sensors or telescope bore-sight calibration (using imagery during science or from regular calibration campaigns) this would simply be the pointing Performance Error of the telescope. The HEW is broken down into several components, e.g.:

- Mirror module internal errors
- Mirror assembly errors (alignment, tilt, focus, structure thermal deformation)
- De-focus due to deviation from nominal focal length
- Relative Knowledge Error (RKE) of Telescope LoS.

The relevant time window for the HEW (image quality) is the image acquisition duration. All errors with frequencies above this time scale will affect the HEW. Corrections of photon positions at these frequencies, using attitude knowledge or centroid measurements from the image, may reduce the HEW but the corrections will still be affected by estimation errors. The worst case time window is defined as Δt, being the longest observation period, up to 100ks. Knowledge errors longer than this time scale will not affect the image quality / HEW.

Note that for most science targets the telescope bore-sight calibration (offset from star tracker frame) can actually be done using centroiding of identified sources in the science image itself to properly superimpose data accumulated during an observation (could be split into segments with regular computation of the centroid correction). This has been mentioned as a strategy and the achievable accuracy is summarized in the picture below (from 'Athena Source Centroiding' memo):

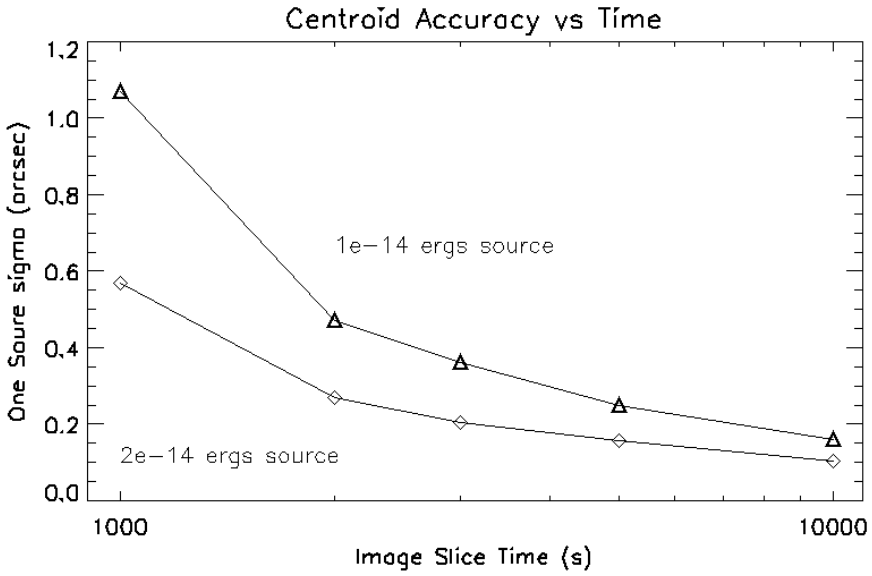

Figure 32: Centroid accuracy vs time for 2 sources with different brightness

The data in the figure above are for one source only. With multiple sources the reduction in systematic errors for pathological source locations and rotations should further improve calibration accuracy.

There is a trade-off to be made between which error frequency band should be addressed by centroiding or AOCS and which band should be addressed by constraining thermos-elastic deformations. With this concept, the RKE requirement on the telescope LoS can be allocated to three sub-contributors:

- Centroiding residual errors from timescales of 100ks to 2ks
    - Error in calibration algorithm and hardware limitations (perhaps of order 1 arcsec, limited by pixel size and calibration technique)
- Relative knowledge error of the LoS from timescales of 2ks to the Nyquist frequency of the star tracker (≈5Hz)
    - Thermoelastic deviation in the star tracker to telescope alignment (between centroiding corrections)
    - Star tracker error
- Platform jitter above the Nyquist frequency of STR frequency
    - E.g. microvibrations, due to the reaction wheels or cryo-coolers.

This is illustrated below in a conceptual power spectral density diagram:

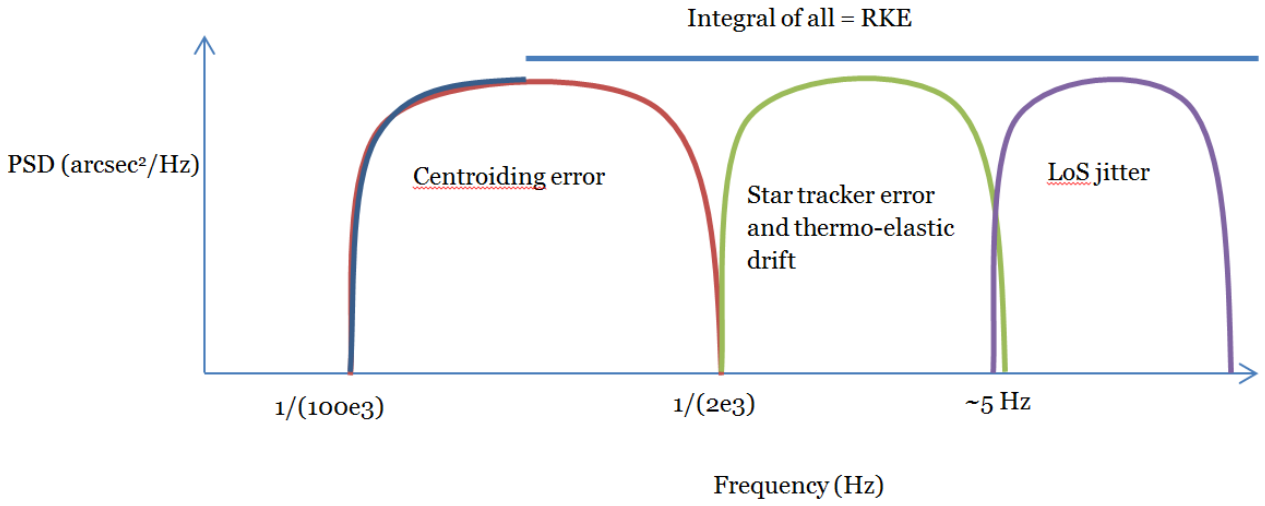

Figure 33: conceptual PSD for RKE allocation to 3 sub-contributors

13.6.2 Relative Knowledge Error (RKE)

Note: The RKE is a contributor to, and therefore derived from, the image quality (HEW) requirement, which is entirely passed to the SC (i.e. it is a SC budget). Consequently it is anticipated that the RKE requirement shall be derived by the SC Prime, and several routes to satisfying the HEW requirement can be envisaged, with differing consequences for the RKE requirements imposed on the SC (e.g. using an active-focusing mechanism).

13.6.2.1 Defining RKE

A requirement on the "Knowledge Error of Telescope LoS (above frequency f)" can be written in ESA standards language as: "The Relative Knowledge Error (RKE) of each telescope's pointing for targets across the entire field of view [only if applicable] over a duration of TBD s shall be less than TBD arcsec at TBD % confidence, using the temporal statistical interpretation."

The RKE refers to the difference in absolute knowledge error (AKE) and mean knowledge error (MKE) over a specified time window Δt (see ECSS-E-ST-60-10C); RKE = AKE – MKE = Absolute Knowledge Error – Mean Knowledge Error (over period t). The temporal statistical interpretation means that it shall meet the requirement TBD % of the time.

13.6.2.2 Using RKE

The reason to define a Relative Knowledge Error (RKE) instead of an Absolute Knowledge Error (AKE) is because to get a low HEW and hence a high quality image the Mean Knowledge Error (MKE) over the duration that the photons were accumulated is not important.

This means that some photons could be collected at the beginning of the observation time window Δt and the end of the window and they could be superimposed to form an image with low HEW as long as (ignoring other HEW contributors) the knowledge error of the

telescope LoS over all frequencies > 1/(Δt) is properly constrained by an RKE requirement. If during the entire observation there was a constant LoS knowledge error of 1 arcmin (for example) it doesn't affect the quality of the image, since all photons in this accumulated image will share this same bias in the correction of their positions using the star tracker data.

13.6.2.3 Confidence level of the requirement

In order to comply with the HEW budget, the LoS shall collect 50% of the photons from point source within the required circle. This translates into a requirement for the LoS being pointed for 50% of the time to the target point source.

The requirement therefore shall have temporal statistical interpretation and confidence level of 50%. In order to translate this into a per axis pointing requirement, we assume the error having a bivariate normal distribution (Gaussian in both directions) with same standard deviation in both directions and zero mean. With such an assumption, given the standard deviation sigma, the range within which a point can fall with probability of 50% is equivalent to ≈2.35σ. This means that HEW requirement can be interpreted as 2.35σ confidence level.

13.6.3 Derived Requirements

The variation of the knowledge in the time window Δt=100ks of the observation will have a direct impact on the reconstructed photon position (image blurring). In pitch and yaw (RKExy) this will translate directly into a PSF degradation of the same magnitude.

In roll, (RKEz) this will to first order have no effect on the HEW of a source located at the centre of the FoV. However for objects further out in the FoV, RKEz will have a more pronounced impact. The MRD requirement is to maintain the HEW to 10" at 25' off-axis, which implies the use of a W-S telescope but does not explicitly take into account blurring effects due to RKE. The contribution HEWz to the PSF for an object 25' from the LoS can be expressed as function of the RKEz, such that:

$$25' \times \tan RPE_z = contribution\ to\ HEW\_z$$

Note: The final FoV of the WFI instrument will determine this mapping. Note that the statistical level shall be scaled to get the correct HEW CL.

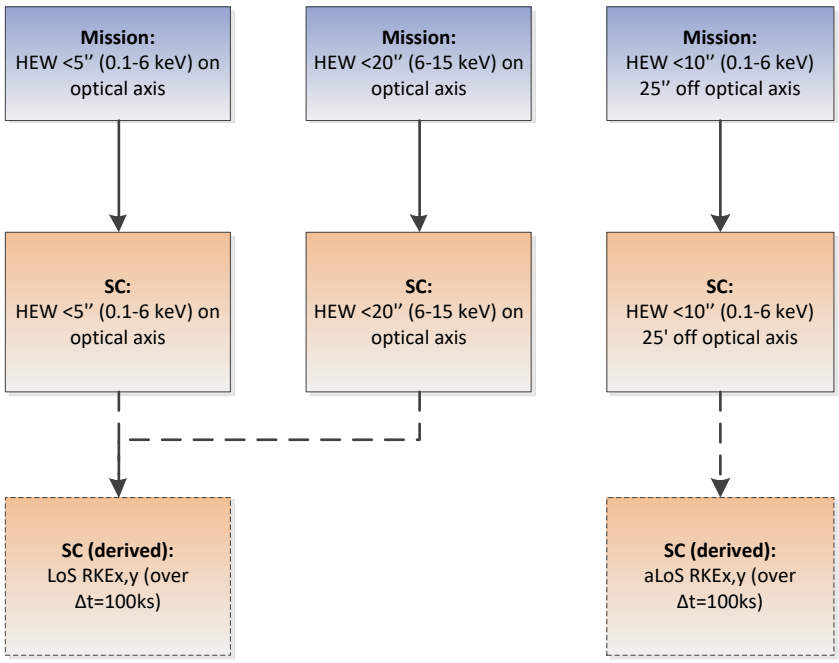

Figure 34: HEW requirements decomposition

14 DELTA V BUDGET (STATION-KEEPING)

14.1 Motivation

Most line-items in the ΔV budget are defined in the CReMA [RD25], with the exception of the station-keeping and safe-mode ΔV during the operational phases, which must be calculated as a function of the assumed limit on SC noise, the frequency of Safe Mode events, and the mission duration. Furthermore the margins to be applied are not defined in the CReMA.

14.2 Decomposition

Assuming that manoeuvre accuracy and orbit determination requirements are met, the ΔV budget for the ATHENA SC station-keeping and safe-mode during the operational phases is a function of the SC non-gravitational acceleration standard deviation, the NoP and EoP durations, and the budgeted number of safe-mode events.

Three simulation cases to determine the required yearly station keeping ΔV are reported in the CReMA, corresponding to different assumptions on the SC ECV (for different perturbation environments and predictability of the parasitic ΔV):

- Case 1: Balanced thruster configuration with no residual ΔV caused by attitude manoeuvres. The simulation has therefore little non-gravitational acceleration. Different standard deviation values for the variation of the solar radiation pressure are discussed.
- Case 2: Unbalanced thruster configuration with predictable ΔV. Noise is assumed on the deterministic ΔV.
- Case 3: Unbalanced thruster configuration with arbitrary ΔV (Herschel case).

An additional case simulates the additional ΔV needed for Safe Mode events:

- Case 4: Special event cases as e.g. safe mode or required re-pointing.

Dependant on the proposed SC design and the mission duration, the required ΔV allocation for a nominal mission can be defined from these simulation results. As required by the CReMA, this decomposition uses an extrapolation from a specific noise case value for the station-keeping or Safe-Mode ΔV until the ΔV value for the next case is reached.

- The worst-case 'Maximum ΔV per year' (sub-case #-3 for each case) for each of the cases defined above (the three data points on Figure 36). This corresponds to auto-correlation times for ECV of 1, 5 and 100 days, and 10% standard deviation for the reflectivity coefficient with an auto-correlation time of 100 days. We then multiply by the NoP duration.
- The worst-case 'ΔV per safe mode' (the three data points on Figure 37) assuming an occurrence of the safe mode at the worst case time and with a worst case duration. We then multiply by the NoP duration and number of Safe Mode events per year.

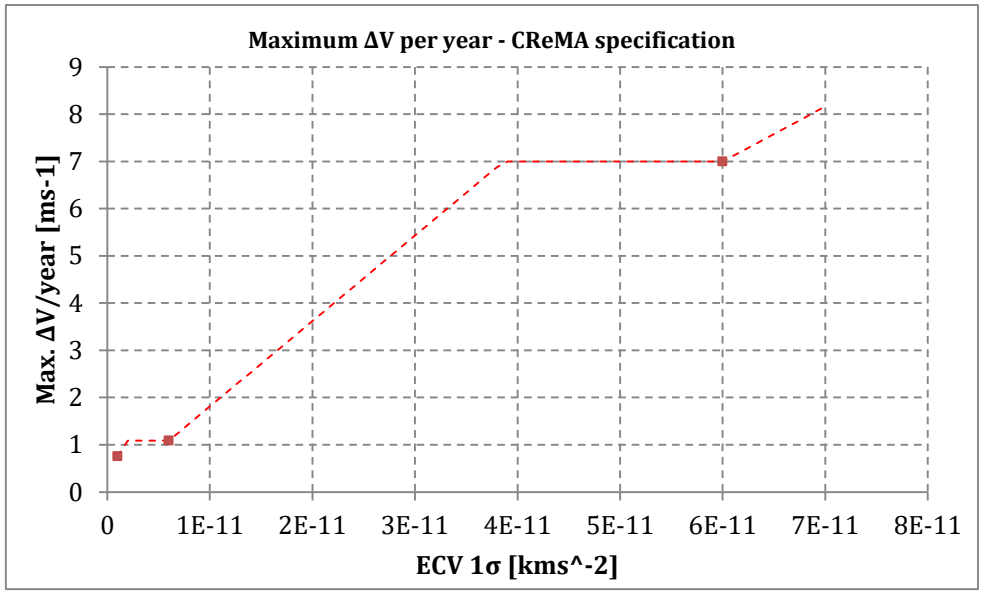

Figure 35: Worst-case maximum ΔV per year

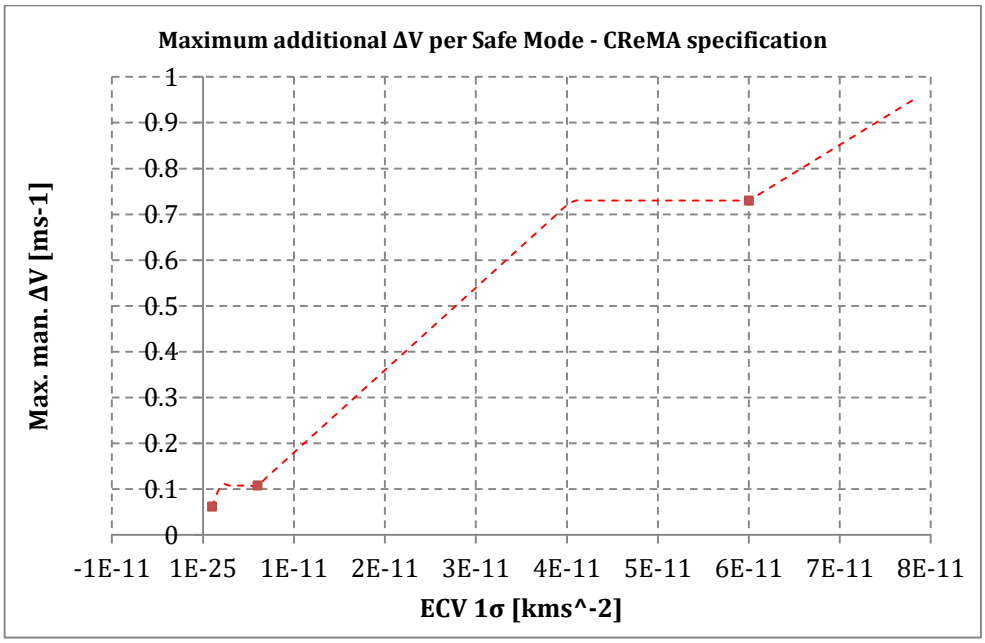

Figure 36: Worst-case additional ΔV per Safe Mode

In addition to the values taken from the CReMA analysis, we define the additional parameters SC system-noise, NoP, EoP durations, and # of Safe-Mode events per year (2).

Table 13: ΔV budget input parameter definition

Parameter	Value
ECV_SC 1σ [km.s^-2]	1.00E-11
Selected Number of Safe Modes [#/year]	2
Nominal Operations Phase Duration [years]	5
Extended Operations Phase Duration [years]	5
ΔV_m1 [m.s^-1]	0.248
ΔV_m2 [m.s^-1]	0.329
ΔV_m3 [m.s^-1]	1.566
ΔV_s1 [m.s^-1]	0.062
ΔV_s2 [m.s^-1]	0.108
ΔV_s3 [m.s^-1]	0.73
ECV_1 [km.s^-2]	1E-12
ECV_2 [km.s^-2]	6E-12
ECV_3 [km.s^-2]	6E-11

$$\Delta V\_SK_{ECV_{SC}} = \begin{cases} \min\left(\frac{ECV_{sc}}{ECV_1}.\Delta V_{m1}, \Delta V_{m2}\right).T_N, & ECV_1 \le ECV_{SC} < ECV_2 \\ \min\left(\frac{ECV_{sc}}{ECV_2}.\Delta V_{m2}, \Delta V_{m3}\right).T_N, & ECV_2 \le ECV_{SC} < ECV_3 \\ \left(\frac{ECV_{sc}}{ECV_3}.\Delta V_{m3}\right).T_N, & ECV_3 \le ECV_{SC} \end{cases}$$

$$\Delta V\_SM_{ECV_{SC}} = \begin{cases} \min\left(\frac{ECV_{sc}}{ECV_1}.\Delta V_{s1}, \Delta V_{s2}\right).SM_{year}.T_N, & ECV_1 \le ECV_{SC} < ECV_2 \\ \min\left(\frac{ECV_{sc}}{ECV_2}.\Delta V_{s2}, \Delta V_{s3}\right).SM_{year}.T_N, & ECV_2 \le ECV_{SC} < ECV_3 \\ \left(\frac{ECV_{sc}}{ECV_3}.\Delta V_{s3}\right).SM_{year}.T_N, & ECV_3 \le ECV_{SC} \end{cases}$$

With similar expressions for the EoP. The selected implementation is to restrict the SC noise standard deviation to $ECV_{SC} = 1.10^{-11} km.s^{-2}$, resulting in the following overall ΔV budget. The margins to be applied in the budget are also specified, along with an additional Operational Contingency allocation.

Note: if the Prime wishes to use a lower SC noise, analysis must be provided to demonstrate that this is achievable.

Table 14: ΔV budget corresponding to ECV_1

Manoeuvre	dV [m.s^-1]	Type	Margin [%]	Margin [m/s]	Total
Transfer					
TCM#1 (perigee velocity correction)	12.7	Deterministic	10%	1.3	14.0
TCM#1 (LV dispersion correction)	36.3	Stochastic	0%	0	36.3
TCM#2	2.47	Stochastic	0%	0	2.47
TCM#3	0.24	Stochastic	0%	0	0.24
Station-keeping					
Nominal Operations Phase	9.05	Orbit Maintenance	100%	9.05	18.1
Extended Operations Phase	9.05	Orbit Maintenance	100%	9.05	18.1
Safe-Mode events (NoP)	1.80	Orbit Maintenance	100%	1.8	3.6
Safe-Mode events (EoP)	1.80	Orbit Maintenance	100%	1.8	3.6
Operational Contingency	10	Stochastic	0%	0	10
Disposal					
Disposal manoeuvre	10	Stochastic	0%	0	10
Total	93.41			23.0	116.4

Note: Once the SC design for ATHENA matures and becomes more defined, the actual propulsion system can be simulated. This could in some cases further reduce the station keeping ΔV requirements.

14.3 Derived Requirements

The requirement has been broken to the SC as follows:

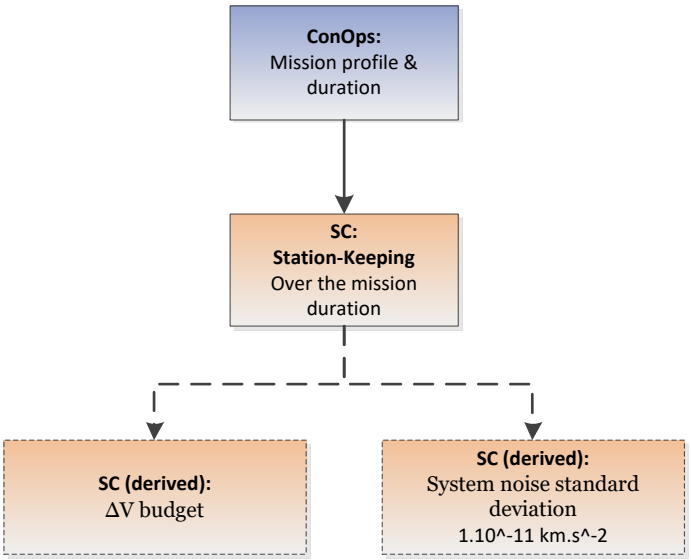

Figure 37: Station-keeping ΔV decomposition